









Evidence for Succession and Putative Metabolic Roles of Fungi and Bacteria in the Farming Mutualism of the Ambrosia Beetle *Xyleborus affinis*

L. A. Ibarra-Juarez,^a M. A. J. Burton,^a  P. H. W. Biedermann,^b L. Cruz,^c  D. Desgarennès,^d  E. Ibarra-Laclette,^a  A. Latorre,^{e,f} A. Alonso-Sánchez,^a E. Villafan,^a G. Hanako-Rosas,^a L. López,^a M. Vázquez-Rosas-Landa,^a G. Carrion,^d D. Carrillo,^d  A. Moya,^{e,f}  A. Lamelas^a

^aRed de Estudios Moleculares Avanzados, Instituto de Ecología A. C., Xalapa, México

^bChair of Forest Entomology and Protection, University of Freiburg, Freiburg, Germany

^cTropical Research and Education Center, University of Florida, Homestead, Florida, USA

^dRed de Biodiversidad y Sistemática, Instituto de Ecología A. C., Xalapa, México

^eInstitute for Integrative Systems Biology (Universitat de València and CSIC), València, Spain

^fFoundation for the Promotion of Sanitary and Biomedical Research in the Valencian Community (FISABIO), València, Spain

L. A. Ibarra-Juarez, M. A. J. Burton, and P. H. W. Biedermann contributed equally to this work. Author order was determined by drawing straws.

ABSTRACT The bacterial and fungal community involved in ambrosia beetle fungi-culture remains poorly studied compared to the famous fungus-farming ants and termites. Here we studied microbial community dynamics of laboratory nests, adults, and brood during the life cycle of the sugarcane shot hole borer, *Xyleborus affinis*. We identified a total of 40 fungal and 428 bacterial operational taxonomic units (OTUs), from which only five fungi (a *Raffaelea* fungus and four ascomycete yeasts) and four bacterial genera (*Stenotrophomonas*, *Enterobacter*, *Burkholderia*, and *Ochrobactrum*) can be considered the core community playing the most relevant symbiotic role. Both the fungal and bacterial populations varied significantly during the beetle's life cycle. While the ascomycete yeasts were the main colonizers of the gallery early on, the *Raffaelea* and other filamentous fungi appeared after day 10, at the time when larval hatching happened. Regarding bacteria, *Stenotrophomonas* and *Enterobacter* dominated overall but decreased in foundresses and brood with age. Finally, inferred analyses of the putative metabolic capabilities of the bacterial microbiome revealed that they are involved in (i) degradation of fungal and plant polymers, (ii) fixation of atmospheric nitrogen, and (iii) essential amino acid, cofactor, and vitamin provisioning. Overall, our results suggest that yeasts and bacteria are more strongly involved in supporting the beetle-fungus farming symbiosis than previously thought.

IMPORTANCE Ambrosia beetles farm their own food fungi within tunnel systems in wood and are among the three insect lineages performing agriculture (the others are fungus-farming ants and termites). In ambrosia beetles, primary ambrosia fungus cultivars have been regarded essential, whereas other microbes have been more or less ignored. Our KEGG analyses suggest so far unknown roles of yeasts and bacterial symbionts, by preparing the tunnel walls for the primary ambrosia fungi. This preparation includes enzymatic degradation of wood, essential amino acid production, and nitrogen fixation. The latter is especially exciting because if it turns out to be present *in vivo* in ambrosia beetles, all farming animals (including humans) are dependent on atmospheric nitrogen fertilization of their crops. As previous internal transcribed spacer (ITS) metabarcoding approaches failed on covering the primary ambrosia fungi, our 18S metabarcoding approach can also serve as a template for future studies on the ambrosia beetle-fungus symbiosis.

Citation Ibarra-Juarez LA, Burton MAJ, Biedermann PHW, Cruz L, Desgarennès D, Ibarra-Laclette E, Latorre A, Alonso-Sánchez A, Villafan E, Hanako-Rosas G, López L, Vázquez-Rosas-Landa M, Carrion G, Carrillo D, Moya A, Lamelas A. 2020. Evidence for succession and putative metabolic roles of fungi and bacteria in the farming mutualism of the ambrosia beetle *Xyleborus affinis*. mSystems 5:e00541-20. <https://doi.org/10.1128/mSystems.00541-20>.

Editor Sarah M. Hird, University of Connecticut

Copyright © 2020 Ibarra-Juarez et al. This is an open-access article distributed under the terms of the [Creative Commons Attribution 4.0 International license](https://creativecommons.org/licenses/by/4.0/).

Address correspondence to A. Moya, andres.moya@uv.es, or A. Lamelas, araceli.lamelas@inecol.mx.

Received 16 June 2020

Accepted 28 August 2020

Published 15 September 2020

KEYWORDS microbiome, mycobiome, *Xyleborus affinis*

Many arthropods, especially insects and mites, engage in symbiotic mutualisms with fungi (1). Only three insect lineages have convergently evolved to farm fungi for nutritional purposes (i.e., advanced fungiculture): fungus-farming termites, attine ants, and ambrosia beetles (1, 2). Farming involves the selection of beneficial fungi over less beneficial (or antagonistic) fungi, a task that is more easily managed by groups of individuals exhibiting division of labor (3). For ants and termites, it has been shown that bacteria play a prominent role in the farming practices (4), in particular by defending the fungal crops against pathogens (5, 6) but also by nitrogen fertilization of fungus cultivars (7, 8) as well as the enzymatic degradation of plant biomass (9, 10) and plant defenses (11).

Ambrosia beetles (Curculionidae: Scolytinae and Platypodinae) are a polyphyletic group of at least 11 independently evolved wood-boring weevil lineages and are defined by an obligate nutritional dependency on fungi (“ambrosia fungi”), farmed in self-bored tunnels within the xylem of trees (12). The most species-rich lineage of ambrosia beetles belong to the scolytine tribe Xyleborini, with several thousand species (12). Species in this lineage are all haplodiploid, and mating is almost exclusively through inbreeding in the natal nest. Some Xyleborini species are among the most advanced fungus farmers, reflected by cooperative breeding found in these species (13, 14). Cooperative breeding in Xyleborini is characterized by division of labor between mothers (= nest foundresses), adult females, and larval offspring. Adults engage in nest protection and brood and fungus care, whereas larvae take over nest cleaning and expansion (13, 15, 16). Many of these behaviors might involve the application of “bacterial helpers” that might fertilize gardens (e.g., by nitrogen fixation), assist the fungal crops with detoxification of plant defensive compounds and degradation of plant cell walls (e.g., by enzyme production) or defense against pathogens (e.g., by antibiotic production). All these functions have been found to be undertaken by bacterial symbionts in related, phloem-feeding bark beetles (4, 17–21).

Ambrosia beetles bore tunnel systems (= galleries) in the xylem of unhealthy or recently dead trees. On their tunnel walls, they cultivate monocultures of mutualistic ambrosia fungi that grow among a background microbiota of other filamentous fungi, yeasts, and bacteria. Visually (both macro- and microscopically), ambrosia fungi dominate in occupied and active nests and the beetles seem to pick out unwanted fungi and keep the ambrosia cultures pure (22–25). All the other microorganisms in the background are more subtle and almost always ignored by researchers except to mention that they “take over” when the farms are abandoned (13, 15, 23). Whereas ambrosia fungi are transmitted from the natal nest to new nests by nest foundresses in specialized spore-carrying organs, termed mycetangia, and only rarely within the gut (26–28), other microbial associates are found only rarely in mycetangia but are instead transmitted in the gut or on the beetle’s surface. Environmental acquisition from the substrate is also possible (but not in the laboratory assay used in this study). The roles of the symbionts are poorly understood, but symbiont communities certainly comprise beetle mutualists and antagonists. Proven nutritional mutualists are the so-called ambrosia fungi in the ascomycete orders Ophiostomatales (e.g., genus *Raffaelea*), Microascales (e.g., genus *Ambrosiella*), and less frequently, Hypocreales (1, 12, 25). Each genus of ambrosia fungi is typically associated with a specific lineage of beetles and a specific type of mycetangia (29–31). Within these lineages, some beetle species can exchange their primary ambrosia fungi (32, 33), whereas others do appear to have species-specific mutualisms (e.g., reference 29). Saccharomycete yeasts have been found in species-specific relationships with scolytine ambrosia beetles of the genus *Xyleborus* (including our study species *X. affinis*), a genus that often shows only unspecific relationships with *Raffaelea* ambrosia fungi (32). Therefore, a coevolved mutualistic or parasitic role for these yeasts is possible in *Xyleborus* ambrosia beetles but currently unproven.

Previous studies have indicated that fungal communities of ambrosia beetles are dynamic, both spatially within their galleries and temporally throughout development with the relative abundances of the different symbionts changing over time (34–38). A succession of different fungal (and bacterial) species should be expected, because as the gallery matures, the surrounding wood substrate dries out and is probably degraded by fungal enzymes (39). Larvae may depend on different symbionts than adults, and control over symbionts in their nests and within their bodies (i.e., mycetangium) is particularly important for nest-founding females just prior to emergence, as they need to transmit the beneficial “starter cultures” from the natal nest. Whether the beetles are able to influence symbiont communities and their succession within galleries is unknown, but some evidence suggests that they can. Both larvae and adults have been shown to (i) hinder the spread of experimentally introduced fungal antagonists (13, 15) and (ii) promote the growth of fungal mutualists (40, 41). The mechanisms by which beetles are able to affect fungal growth are still unknown, but they may involve mechanical removal, oral secretions, and the application of mutualistic bacteria (15, 20, 42). Symbiont communities within their bodies and particularly mycetangial symbionts can certainly be influenced by the beetles, as adult females prior to dispersal are known to activate their mycetangia, which are more or less selective for particular ambrosia fungus taxa (43, 44).

There is a long history of studying fungal and bacterial associates in ambrosia beetles, e.g., by using traditional culturing techniques (32, 34, 36–38, 45) or culture-independent approaches (4, 27, 46, 47). Some of these studies have monitored fungal symbionts over time (37, 38, 48–50). Nevertheless, no study has monitored the fungal and bacterial communities associated with all the offspring’s life stages and throughout the development of a beetle gallery using metabarcoding. This kind of study has revealed roles of specific and apparently essential symbionts in leaf-cutter ants, for example (11). In ambrosia beetles, dynamics of symbionts are poorly known, and therefore, we can currently only make guesses about the roles of specific symbionts and their interactions in the development of the beetles.

Here we report the first fungal and bacterial metabarcoding study of the symbiont communities of galleries, gallery foundresses, and offspring of all life stages in the sugarcane shot hole borer, *Xyleborus affinis* Eichhoff. Despite its abundance and pest status (51, 52), microbial symbionts of *X. affinis* remain poorly studied, and the main ambrosia-fungus mutualist(s) have not been determined for this species, even though several candidates like *Raffaelea arxii*, a *Candida* sp., and an *Ambrosiozyma* sp. have been discussed as potential mutualists (32). We used a laboratory rearing technique (53) that allows tracking the development of the beetles and collecting samples of specimen and galleries at specific time points, from particular life stages and from the beetle’s oral mycetangia (Fig. 1). Finally, we predict metabolic functions of the microbial communities by using public metabolic databases.

RESULTS

After quality and chimeric sequence filtering, 5,084,456 bacterial reads and 8,009,205 fungal reads were obtained, with a mean (\pm standard deviation [SD]) of $181,587 \pm 229,231$ bacterial and $29,970 \pm 21,813$ fungal reads per sample (see Table S1 at <https://doi.org/10.6084/m9.figshare.12477593>). The reads were grouped into 428 bacterial operational taxonomic units (OTUs) (97% homology) and 40 fungal OTUs (99% homology).

The 428 bacterial OTUs belonged to eight different phyla (*Acidobacteria* [0.23%], *Actinobacteria* [8.88%], *Bacteroidetes* [10.51%], *Chloroflexi* [0.23%], *Firmicutes* [13.79%], *Proteobacteria* [64.49%], *Tenericutes* [0.23%], and TM7 [0.93%]) (Fig. S1). Bacterial taxonomic cladograms differed between the types of the samples (galleries, foundresses, offspring) (Fig. S1). While *Gammaproteobacteria* (*Enterobacter* and *Stenotrophomonas*) predominated in galleries, *Betaproteobacteria* (*Burkholderiaceae*, *Alcaligenaceae*, and *Comamonadaceae*), *Alphaproteobacteria* (*Sphingomonadaceae* and *Brucellaceae*), *Sphingobacteria* (*Sphingobacterium*), *Bacteroidetes* (*Chryseobacterium*), and *Actinobacteria*

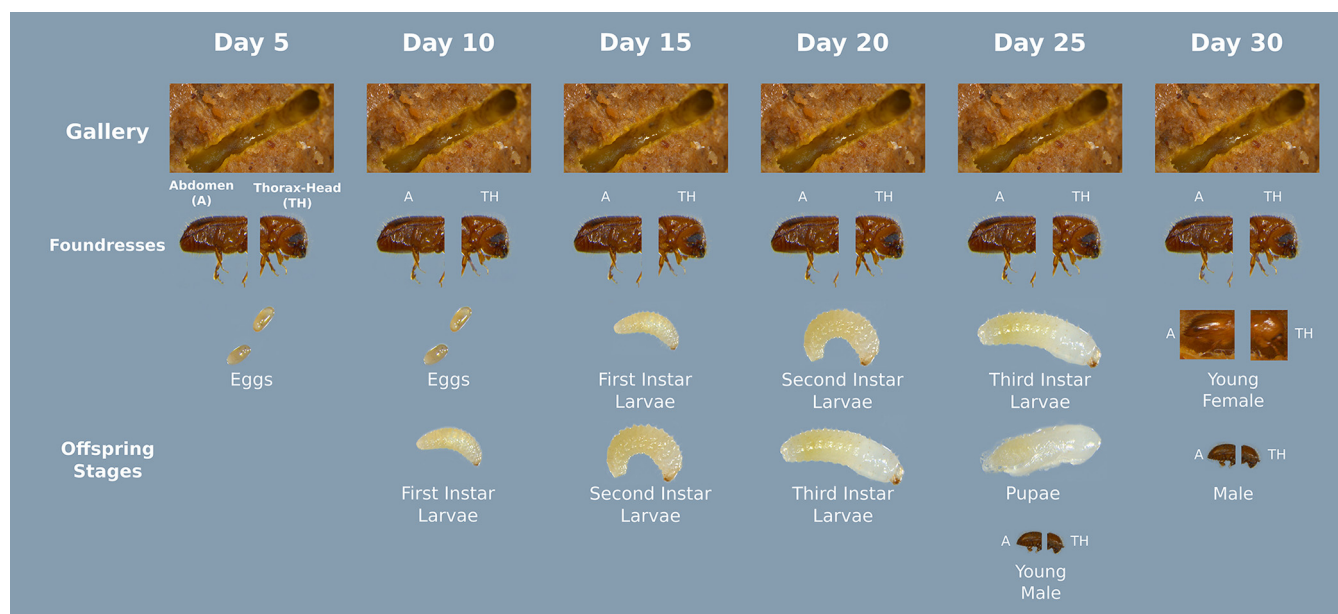


FIG 1 Sample collection and experimental procedure. Six colonies were dissected every 5 days. Samples from the galleries, foundresses, and all offspring at the life stages available at specific time points were collected. The abdomen (A) and thorax-head (TH) were processed independently.

(*Mycobacteriaceae*, *Gordoniaceae*, and *Tsukamurellaceae*) made up the bacteriome of foundresses and offspring, with *Actinobacteria* being the most abundant and diverse in foundresses (Fig. S1).

The fungal OTUs were classified in six orders (Mucorales [5%], Hypocreales [10%], Saccharomycetales [32.5%], Microascales [5%], Ophiostomatales [15%], and Eurotiales [2.5%]) (Fig. S2). The relative abundance of the different taxa in the fungal microbiome also varied between the types of samples (galleries, foundresses, and offspring). While only a few taxa in the Saccharomycetales (*Candida* and *Saccharomycopsis*), Ophiostomatales (*Raffaelea*), Eurotiales (*Talaromyces*), Hypocreales (*Fusarium*), and Mucorales predominated in the galleries, additional Saccharomycetales (plus *Cyberlindnera* and *Meyerozyma*) and Microascales (*Graphium*) dominated in the foundresses and offspring (Fig. S2). Relative abundance measures based on 16S/18S amplicon sequencing analyses have to be treated with care, however, because relative abundances based on ribosomal genes do not directly translate to physical abundance of the specific microbes (54). Semiquantitative comparisons between samples are possible, however.

Overall, both fungal and bacterial OTU richness and diversity varied between samples and throughout beetle development (for details, see Fig. S3 to S8 at <https://doi.org/10.6084/m9.figshare.12477593>).

Structure of fungal and bacterial communities throughout beetle development. The abundance of bacterial and fungal OTUs was strongly biased toward certain taxa (Fig. 2 and 3). Forty-six bacterial OTUs had an abundance of $>1\%$ (Fig. 2). Only five of these OTUs were relatively abundant in all the samples: a *Stenotrophomonas* (OTU 815480; mean \pm SD of $23.9\% \pm 16.1\%$), an *Enterobacter* (OTU 922761; $6.42\% \pm 5.8\%$), an *Ochrobacter* (OTU 2458172; $5.21\% \pm 4.12\%$), a *Chryseobacterium* (OTU 573326; $4.07\% \pm 4.92\%$) and a *Sphingobacterium* (OTU 891031; $4.07\% \pm 4.97\%$). The two most abundant OTUs, an *Enterobacter* and a *Stenotrophomonas*, dominated communities of galleries ($37.4\% \pm 15.9\%$ and $30.8\% \pm 9.2\%$; see Fig. S9 at <https://doi.org/10.6084/m9.figshare.12477593>), heads ($22.11\% \pm 36.93\%$ and $9.76\% \pm 6.31\%$), and abdomens of foundresses ($20.74\% \pm 32.48\%$ and $26.9\% \pm 23.77\%$; see Fig. S10 at the figshare URL above), as well as eggs (29.24% and 20.16%) and first/second larval instars ($12.49 \pm 1.98\%$ and $28.50 \pm 11.45\%$) (see Fig. S11 at the figshare URL above). Both, but in particular *Enterobacter*, changed in frequency along with the beetle's life stages. They

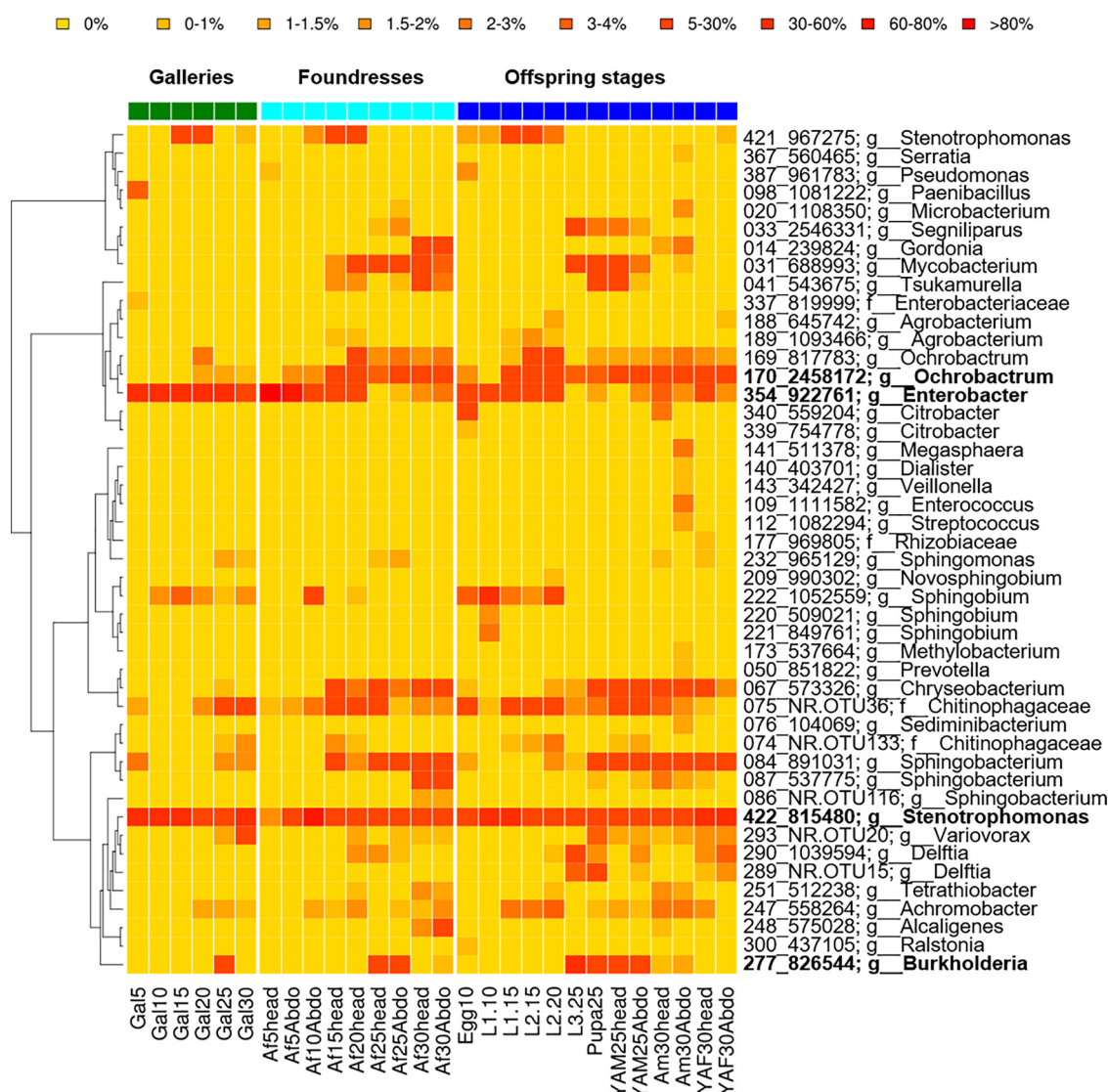


FIG 2 Relative abundances of the 46 most abundant (>0.1%) bacterial OTUs per sample within galleries, foundresses, and offspring of different life stages of *X. affinis*. The predominant bacterial symbionts (abundance of >20% across samples), an *Ochrobactrum* OTU, an *Enterobacter* OTU, a *Stenotrophomonas* OTU, and a *Burkholderia* OTU, are given in bold type. Six samples from each gallery (Gal), foundress (adult female [Af]), and offspring life stage (adult male [Am], teneral female [young adult female {YAF}], teneral male [young adult male {YAM}], pupa, larva first to third instar [L1 to L3], egg; mycetangium [head], abdomen [Abdo]) were pooled and collected between 5 and 30 days after gallery foundation. The dendrogram on the left side shows the 16S phylogenetic relationship between the OTUs.

were rare in third instar larvae, pupae, and young males, in which a *Burkholderia* (OTU 826544; 23.99% \pm 15.94%) and a *Mycobacterium* (OTU 688993; 10.07 \pm 6.15%) OTU predominated. *Enterobacter* was especially abundant within eggs, larvae, and foundresses from young nests.

The relative abundances of the fungal OTUs varied along with the development of galleries and beetle life stages (Fig. 3). Three yeasts (NCR.OTU26209, NCR.OTU14050, and AB054883.1.1755) and two *Raffaelea* OTUs (GenBank accession no. AY497519.1.1318 and JF327799) were widely distributed throughout gallery and beetle samples. Along with gallery development, a *Candida* OTU (AB054883.1.1755) started with a relative abundance of 52.2% at day 5 and decreased down to 1.6% by day 30 (see Fig. S12 at <https://doi.org/10.6084/m9.figshare.12477593>). In contrast, a *Raffaelea* OTU (AY497519.1.1318) was absent in galleries at day 5, reached 19.5% at day 10, and then kept an abundance of around 40%. An unknown Saccharomycetales yeast

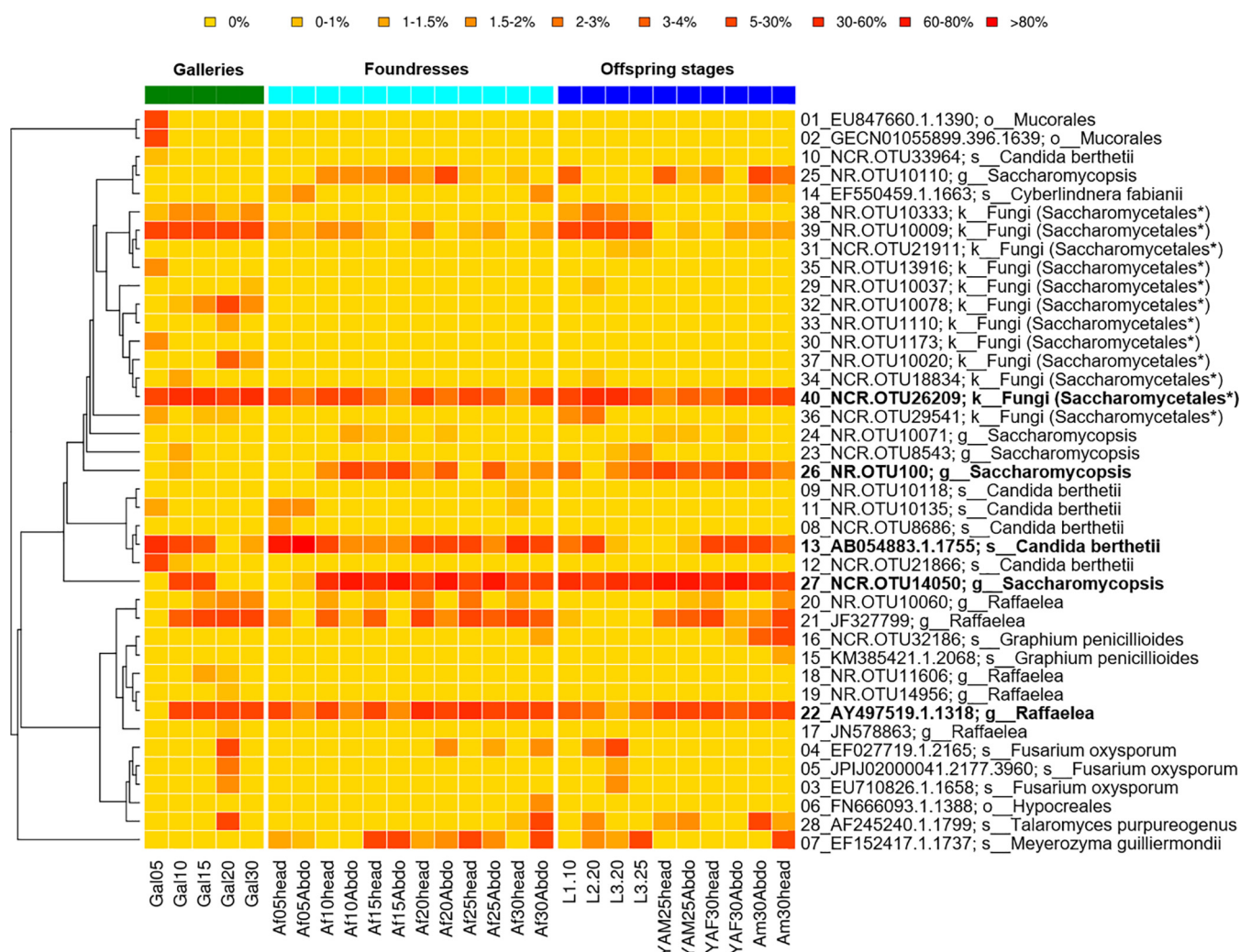


FIG 3 Relative abundance of fungal OTUs per sample within galleries, foundresses, and offspring of the different life stages of *X. affinis*. The predominant fungal symbionts (abundance of >20% across samples), a *Raffaelea* OTU and four OTUs of ascomycete yeasts, are given in bold type. Six samples from each gallery (Gal), foundress (adult female [Af]) and offspring life stages (adult male [Am], teneral female [YAF], teneral male [YAM], larva first to third instar [L1 to L3]; mycetangium [head], abdomen [Abdo]) were pooled and collected between 5 and 30 days after gallery foundation. The dendrogram on the left side shows the 185 phylogenetic relationship between the OTUs. An asterisk shows that these OTUs could not be classified and were automatically assigned to “fungi,” but given their phylogenetic placement, we assigned them to Saccharomycetales.

(NCR.OTU26209) was abundant throughout gallery development ($30.82\% \pm 11.37\%$) and may serve as larval food (see below).

A *Raffaelea* OTU (AY497519.1.1318) growing abundantly in galleries was also commonly found in foundresses ($15.31\% \pm 12.45\%$) and mostly in their heads ($22.89\% \pm 12.92\%$), suggesting that it colonizes the oral mycetangia (see Fig. S13 at <https://doi.org/10.6084/m9.figshare.12477593>). In contrast, larvae mostly lacked this *Raffaelea* OTU ($3.10\% \pm 1.40\%$) but instead contained a *Saccharomycopsis* OTU (NCR.OTU14050; $36.17\% \pm 19.10\%$) and the unknown Saccharomycetales yeast (NCR.OTU26209; $32.14\% \pm 12.20\%$) (see Fig. S14 at the figshare URL above). In addition to the *Raffaelea* OTU (AY497519.1.1318), the heads and abdomens of foundresses were dominated by two yeasts, a *Candida* OTU (AB054883.1.1755) and the larval *Saccharomycopsis* OTU (NCR.OTU14050), both of which relative dominances within foundress samples fluctuated over time (see Fig. S13 at the figshare URL above).

Microscopic analyses. Dynamics of the microbial communities were also visualized using gallery samples for scanning electron microscopy (SEM) and light microscopy (LM) (Fig. 4 and 5; see Fig. S15 to S17 at <https://doi.org/10.6084/m9.figshare.12477593>).

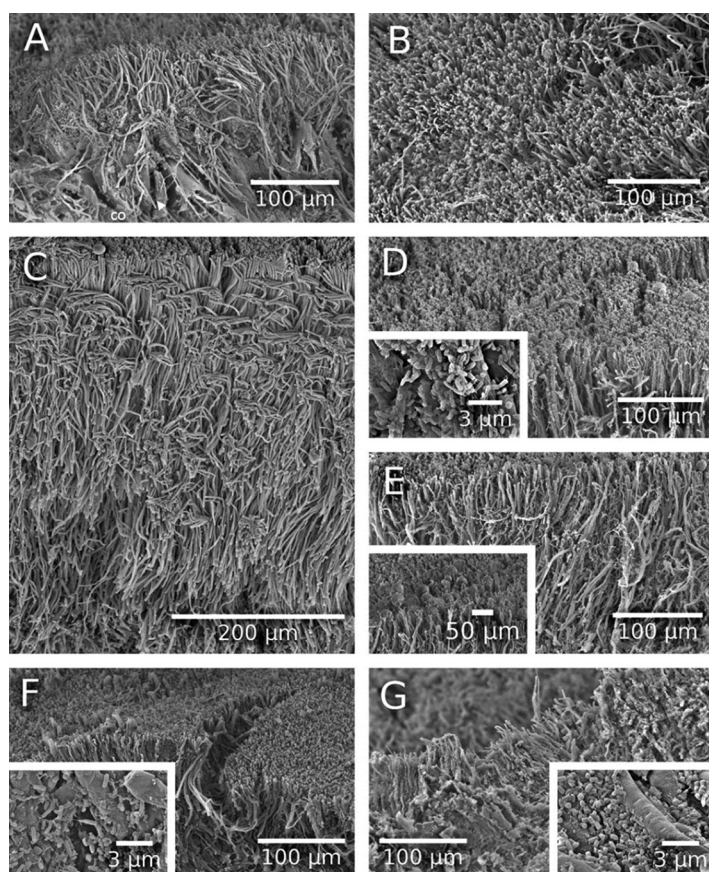


FIG 4 Scanning electron microscopy images of *X. affinis* galleries (1,000 \times magnification, lateral view). (A) Hyphae and yeast-like cells (possibly *Candida*) on day 3, (B to G) mycelium from yeast and ambrosia fungi on (B) day 5, (C) day 10, detached conidium (co), (D) day 15 (bacteria cells, 30,000 \times magnification), (E) day 20 (conidia and conidiophores, 2,500 \times magnification), (F) day 25 (bacteria cells, 30,000 \times magnification), and (G) day 30 (bacteria cells, 30,000 \times magnification). See also Fig. S15, S16, and S17 at <https://doi.org/10.6084/m9.figshare.12477593>.

Shortly, after gallery foundation, between days 5 and 10, both SEM and LM revealed the establishment of filamentous yeast and bacterial communities on gallery walls (Fig. 4A to C and Fig. 5A and B; see Fig. S15A to E at the figshare URL above). Between days 5 and 10, the yeast mycelium grew from $94.06 (\pm 4.49) \mu\text{m}$ by SEM and $95.6 (\pm 5.63) \mu\text{m}$ by LM to its maximum lengths of $379.39 (\pm 10.46) \mu\text{m}$ by SEM and $221.07 (\pm 6.89) \mu\text{m}$ by LM. On day 10, a transition from yeast-like to hyphal growth was observed (see Fig. S15F at the figshare URL above), and the first fungal conidiophores and conidia appeared, resembling those of *Raffaelea* and *Fusarium* species (see Fig. S15D and E at the figshare URL above). On day 15, the bacterial abundance increased along with the production of exopolysaccharides (biofilm) (Fig. 4D and 5C; see Fig. S16A at the figshare URL above). Three different bacterial morphotypes could be observed (Fig. 4D, inset). On day 20, *Raffaelea* conidiophores proliferated on the surfaces of the galleries (Fig. 4E; see Fig. S16B and C and Fig. S17A at the figshare URL above). On day 25, only one bacterial morphotype was detected, and the number of *Raffaelea* conidiophores decreased again (Fig. 4F; see Fig. S16D and E, and Fig. S17B at the figshare URL above). On day 30, signs of mycelial degradation and only one bacterial morphotype were seen (Fig. 4G; see Fig. S16F and Fig. S17B at the figshare URL above). Interestingly, transverse sections of galleries (from both SEM and LM; Fig. 4 and 5; see Fig. S17 at the figshare URL above) revealed that the microbial community on gallery walls is composed of three layers: at the bottom are bacteria, and yeasts, then fungal filaments, and on top, *Raffaelea* conidiophores and conidia that can be also seen in the images taken from the top (Fig. 4; see Fig. S16 at the figshare URL above).

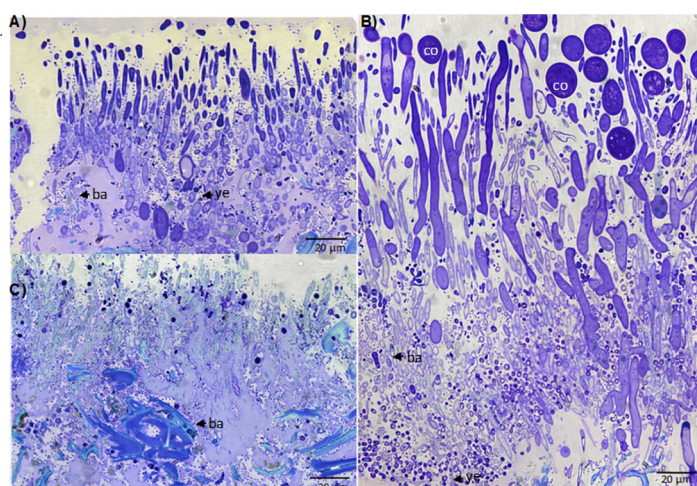


FIG 5 Light microscopy images of transversal sections of tunnel walls through gallery development. (A) Day 5, (B) day 10, (C) day 15. Bacteria (ba), yeast cells (ye), and conidia (co) (possibly *Raffaelea*) are indicated. Magnification, 40 \times .

Putative metabolic function of the microbiota over time. To further investigate the bacterial metabolic shift over time, we predicted the metabolic profile of the samples using PICRUSt software. On the basis of permutational multivariate analysis of variance (PERMANOVA) and nonmetric multidimensional scaling (NMDS) analyses, we found that time (days 5, 10, 15, 20, 25, and 30) and sample type (adult beetles [= foundresses and nonsclerotized offspring], galleries, and immature offspring [= eggs, larvae, and pupae]) determined the metabolic profile of the bacterial community. The PERMANOVA of KEGG functional orthologs (KOs) ($F_{(2, 55)} = 12.03$, $R^2 = 0.32931$, $P = 0.001$) and of L3 KEGG level ($F_{(2, 55)} = 5.08$, $R^2 = 0.20227$, $P = 0.001$) showed significant differences among sample types and also among timing of sampling (for KOs, $F_{(7, 55)} = 5.74$, $R^2 = 0.39233$, $P = 0.001$; for L3, $F_{(7, 55)} = 4.36$, $R^2 = 0.4336$, $P = 0.001$) (see Fig. S18 and details in the supplemental material posted at <https://doi.org/10.6084/m9.figshare.12477593>).

(i) Degradation of the fungal and plant cell wall. The bacterial symbionts together can possibly degrade all the major plant and fungal polymers like chitin, glucan, mannan, cellulose, hemicellulose, pectin, lignin, arabinose, and rhamnose (Fig. 6). A few bacterial OTUs can degrade specific compounds on their own: chitin (*Enterobacter* and *Citrobacter*), glucan (*Pseudomonas*), and pectin (*Serratia*). Cellulose, hemicellulose, lignin, arabinose, and rhamnose can be degraded by many OTUs. The four predominating bacterial taxa possibly have the capabilities to fully degrade all polymers except glucan, mannan, and pectin.

The enzymatic capabilities of the fungal symbionts appear less complete (Fig. 7). Only glucan and mannan can be fully degraded by the joint activity of the fungi. Glucan can be degraded by all fungi, but apart from a *Fusarium* (a relatively uncommon OTU) that possibly has all the genes required for mannan degradation, none of the other symbionts is able to degrade a polymer completely on its own. Among the dominant players, *Raffaelea* is possibly the most potent degrader of plant cells (i.e., cellulose, partly hemicellulose) (Fig. 7).

If putative enzymatic capabilities of OTUs are mapped against sampling time (days 5 to 30) and sample type (adult beetles [= foundresses and nonsclerotized offspring], galleries, and immature offspring [= eggs, larvae, and pupae]), the following pattern appears: cellulose-, hemicellulose-, mannan-, and rhamnose-degrading bacterial symbionts are relatively more abundant during the first half of gallery development (until day 15), whereas symbionts degrading lignin are more abundant during the second half (see Fig. S20 at <https://doi.org/10.6084/m9.figshare.12477593>). During the second half of gallery development, cellulose, hemicellulose, and rhamnose degradation ca-

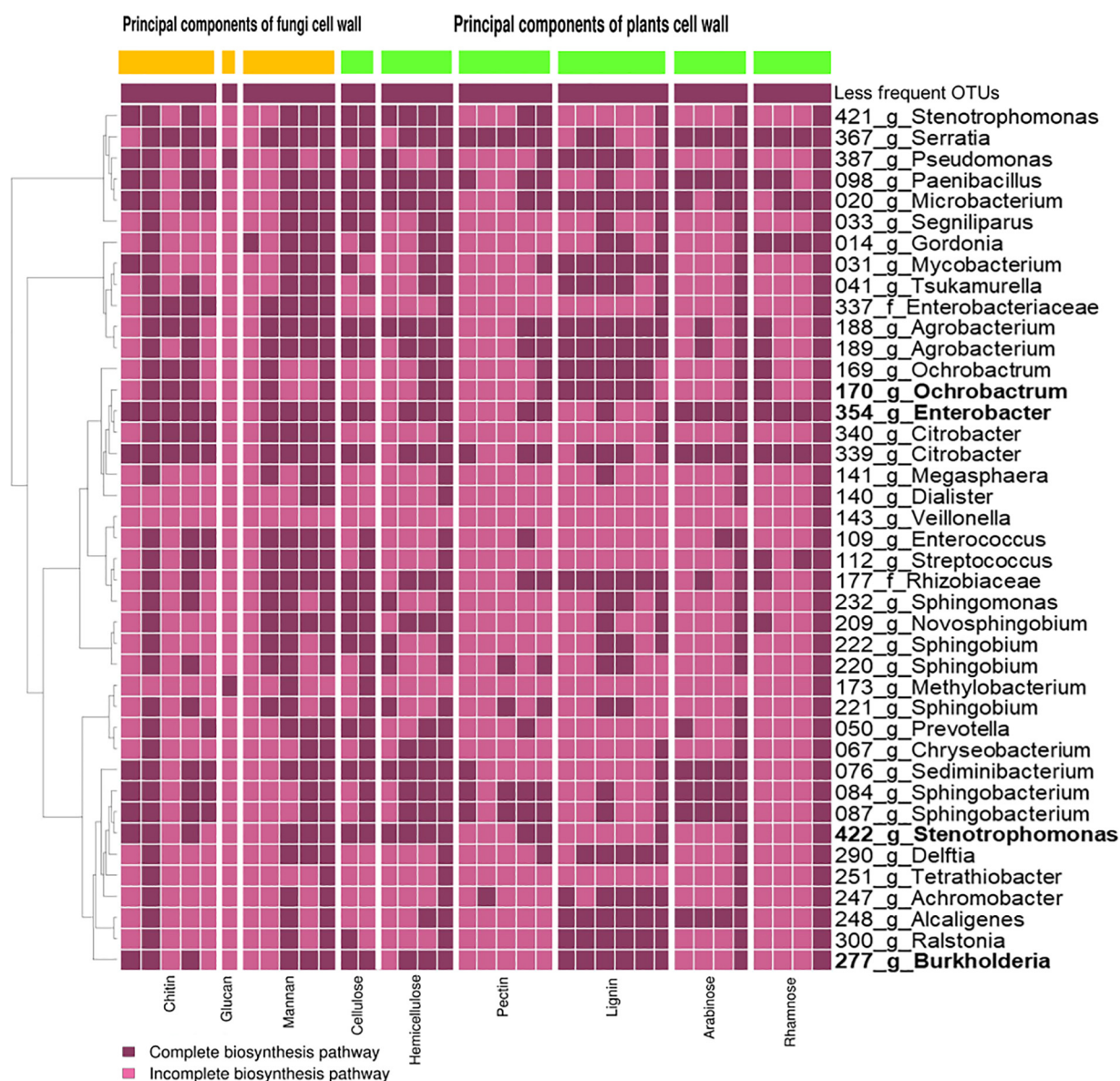


FIG 6 Presence or absence of genes inferred from the KEGG database coding for cell wall-degrading enzymes in the bacterial community found in this study. We display only the OTUs present in the Greengenes database and with a relative frequency of >1% in at least one sample. The predominant bacterial symbionts (abundance of >20% across samples), an *Ochrobactrum* OTU, an *Enterobacter* OTU, a *Stenotrophomonas* OTU, and a *Burkholderia* OTU, are given in bold type. The heatmap shows the presence (dark purple) or absence (light purple) of the catabolic enzymes required for the degradation of a given cell wall component. Every column stands for an individual enzyme required to degrade the respective compound (for details, see Fig. S35 and Table S6 at <https://doi.org/10.6084/m9.figshare.12477593>). The dendrogram on the left side shows the 16S phylogenetic relationship between the OTUs.

pabilities are highest on day 30. Cellulose-, hemicellulose-, and mannan-degrading capabilities are more common in symbionts within galleries than in symbionts of adults and immature offspring; the reverse pattern appears for lignin and glucan (see Fig. S21 at the figshare URL above). The dominant genera *Enterobacter*, *Stenotrophomonas*, and *Ochrobactrum* as well as the relatively abundant *Sphingobacterium*, probably play the main role in the degradation of complex sugars (see Fig. S22 and S23 at the figshare URL above).

(ii) Nitrogen fixation and biosynthesis of amino acids, cofactors, and vitamins.

Atmospheric nitrogen fixation is only known from bacteria, not fungi. Among the predominant bacterial symbionts, an *Enterobacter* can possibly fix nitrogen. Additionally, there might be nitrogen fixation by a *Sphingobacterium*, a *Sphingomonas*, and a

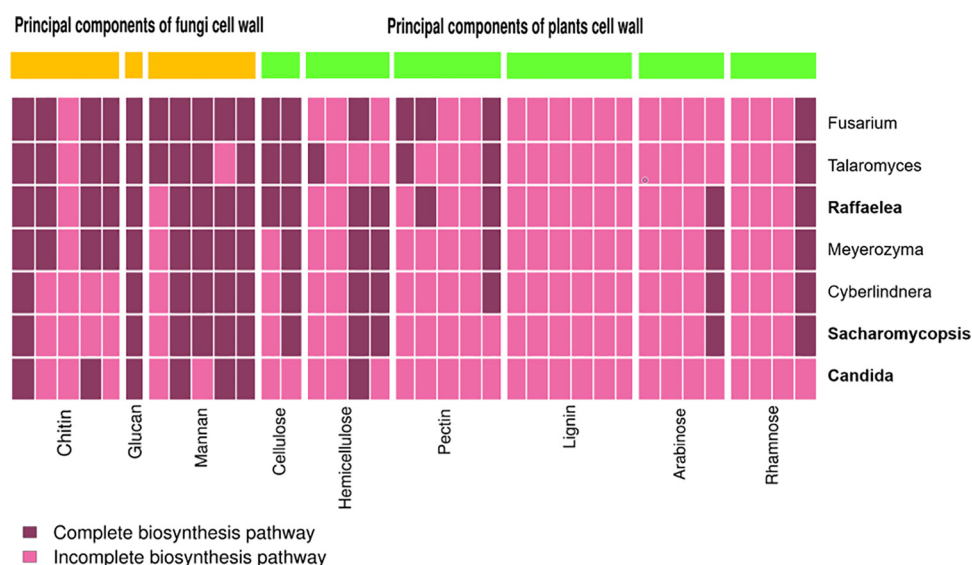


FIG 7 Presence or absence of genes, inferred from fungal genome comparisons, coding for cell wall-degrading enzymes for a subset of the fungal community found in this study. The predominant fungal symbionts (abundance of >20% across samples), a *Raffaelea* strain, a *Saccharomycopsis* strain, and a *Candida* strain, are given in bold type. The heatmap shows the presence (dark purple) or absence (light purple) of the specific enzymes required for the degradation of a given cell wall component. Every column stands for an individual enzyme required to degrade the respective compound (for details, see Fig. S36 and Table S6 at <https://doi.org/10.6084/m9.figshare.12477593>).

Methylobacterium, but all these were uncommon within the microbiome (Fig. 8). Altogether, these taxa were relatively more abundant in galleries than in adults and immature offspring, and immediately after nest foundation, their abundance decreased (see Fig. S24 and S25 at <https://doi.org/10.6084/m9.figshare.12477593>).

Regarding essential amino acids, almost all bacterial OTUs can possibly synthesize them except for histidine, which can be only synthesized by 13 OTUs and only two of the most abundant bacterial OTUs (*Enterobacter* and *Stenotrophomonas*) (Fig. 8).

The fungal symbionts altogether are likely not able to synthesize methionine (either EC 2.3.1.46 or EC 2.3.1.31 is absent). Fungal OTUs with capabilities for synthesis of isoleucine, valine, leucine, and threonine increased in abundance along with the progression of the beetle's life cycle and were generally higher in adults and in immature offspring than in gallery samples (see Fig. S24 and S25 at <https://doi.org/10.6084/m9.figshare.12477593>). In contrast, OTUs with the capability to produce tryptophan and methionine decreased with development of galleries and were also less common in adults and immature offspring than in gallery samples.

The core fungi *Raffaelea*, *Saccharomycopsis*, and *Candida* possibly lack the genes encoding components needed to synthesize tryptophan, riboflavin, pantothenate, biotin, and folate (Fig. 9). Overall, the nine dominant bacterial and fungal symbionts may jointly synthesize 14 out of the 16 cofactors and vitamins (except riboflavin and menaquinone).

Maximum synthesis of thiamine, vitamin B6, coenzyme A (CoA), biotin, lipoic acid, folate, and the one-carbon pool by folate, siroheme, and heme appears to occur around the first half of gallery development (until day 15) and on day 30, with the exception of siroheme (see Fig. S26 and S27 at <https://doi.org/10.6084/m9.figshare.12477593>). The biosynthesis of nicotinate and nicotinamide peaked on day 5 and day 30, mainly in galleries for nicotinamide and in adult beetles (foundresses and nonsclerotized offspring) for nicotinate (see Fig. S26 and S27 at the figshare URL above). Pantothenate biosynthesis peaked in adult beetles on day 25. The biosynthesis of uroporphyrinogen III increased as the beetles completed their life cycle, exhibiting a peak on day 30 in the immature offspring samples. *Enterobacter*, *Stenotrophomonas*, *Mycobacterium*, *Ochrobactrum*, and *Sphingobacterium* probably played the main role in the amino acid

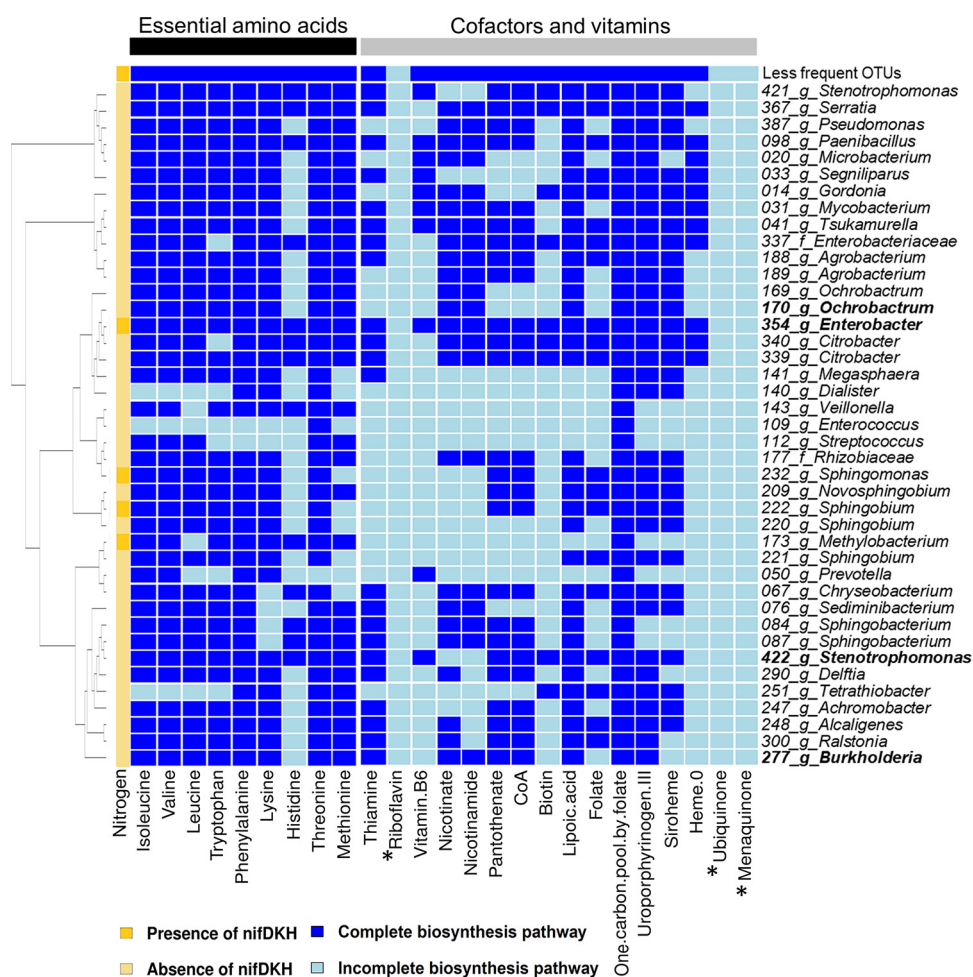


FIG 8 Presence or absence of genes inferred from the KEGG database coding for nitrogen-fixing enzymes, essential amino acids, cofactors, and vitamin biosynthesis pathways in the bacterial community identified in this study. The predominant bacterial symbionts (abundance of >20% across samples), an *Ochrobactrum* OTU, an *Enterobacter* OTU, a *Stenotrophomonas* OTU, and a *Burkholderia* OTU, are given in bold type. The first column shows the presence (dark yellow) or absence (light yellow) of *nifDKH* genes (nitrogenase enzyme complex to fix atmospheric nitrogen). The left heatmap panel shows the amino acid biosynthesis pathways and the right heatmap panel shows cofactors and vitamins biosynthesis pathways (dark blue for complete pathway; light blue for incomplete pathway). Metabolites with an asterisk are not encoded by any bacterial OTU in the microbiome (riboflavin, ubiquinone, and menaquinone). Every column stands for an individual enzyme required to synthesize the molecule. For more details, see Table S6 at <https://doi.org/10.6084/m9.figshare.12477593>. The dendrogram on the left shows the phylogenetic relationships between the OTUs.

synthesis (see Fig. S28 and S29 at the figshare URL above). While *Enterobacter* and *Stenotrophomonas* were highly abundant in all the samples, *Mycobacterium* was present only in adult samples (see Fig. S5 at the figshare URL above).

(iii) Quorum sensing and biofilm production. The analysis of putative quorum-sensing genes in the bacterial symbionts revealed the presence of four complete systems: *Escherichia coli* (*luxS/AI-2* [autoinducer 2]), primarily associated with biofilm production, *Xanthomonas campestris* (*rpfB/rpff/DSF* [diffusible signal factor]), which is associated with virulence and antibiotic resistance and known to induce *Candida albicans* hypha formation (55), *Enterococcus faecalis* (*fsrD/GBAP* [gelatinase bio-synthesis-activating pheromone]) that controls the expression of pathogenicity (56), and enterohemorrhagic *E. coli* (EHEC) (*qseC/AI-3*) known to facilitate the invasion of intestinal epithelia (57) (see Fig. S30 at <https://doi.org/10.6084/m9.figshare.12477593>). The *luxS/AI-2* system is probably carried by the dominant *Enterobacter* and a few other more uncommon genera (*Serratia*, *Microbacterium*, *Citrobacter*, *Enterococcus*, *Streptococcus*, and *Prevotella*). Only *Enterobacter* may contain the sensing proteins (see Fig. S30

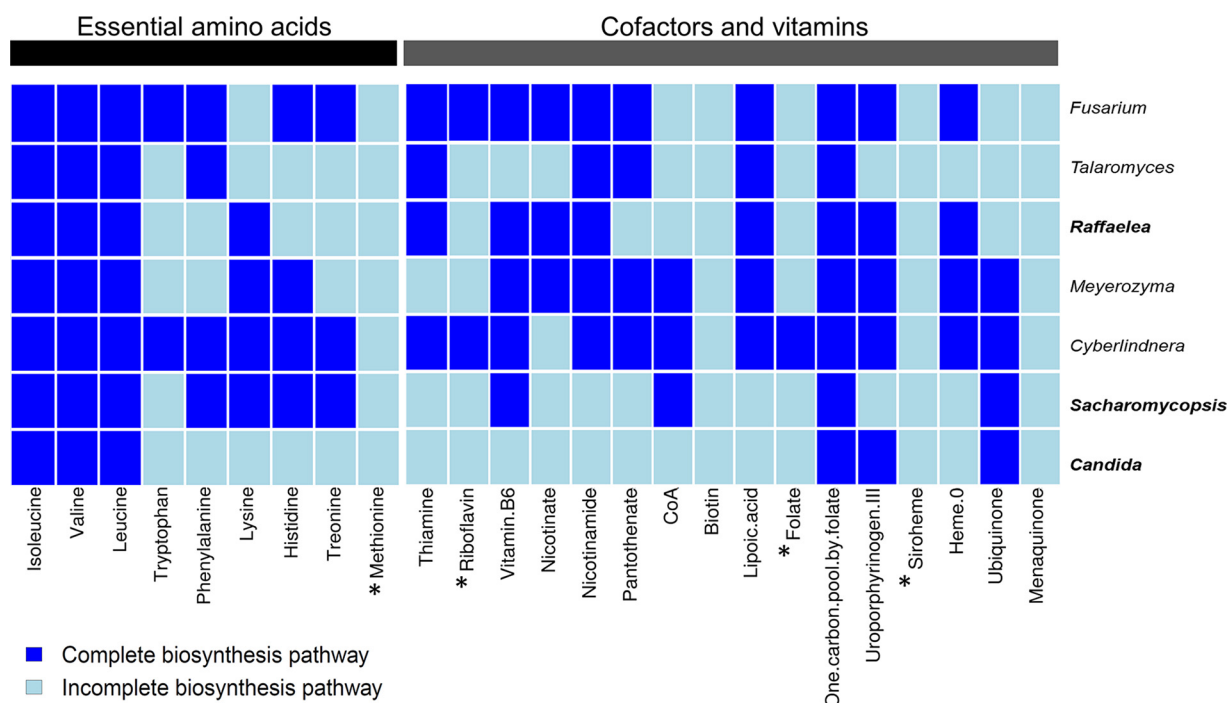
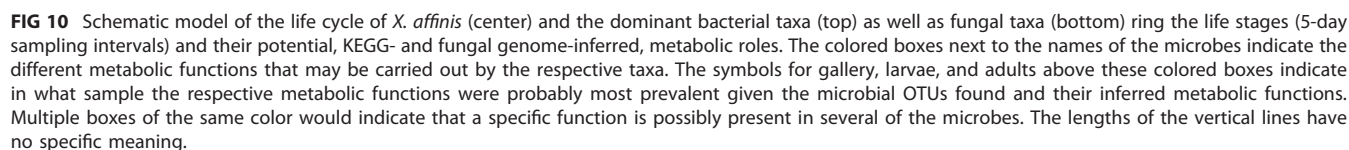


FIG 9 Presence or absence of genes, inferred from fungal genome comparisons, coding for components of biosynthesis pathways of essential amino acids, cofactors, and vitamins in the fungal community identified in this study. The predominant fungal symbionts (abundance of >20% across samples), a *Raffaelea* strain, a *Saccharomycopsis* strain, and a *Candida* strain, are given in bold type. The left heatmap panel shows the amino acid biosynthesis pathways, and the right heatmap panel shows cofactors and vitamins biosynthesis pathways (dark blue for complete pathway; light blue for incomplete pathway). Metabolites with an asterisk lack an enzyme that is not encoded by any fungal OTU in the microbiome (methionine and siroheme). Every column stands for a specific enzyme required to synthesize the molecule. For more details, see Table S6 at <https://doi.org/10.6084/m9.figshare.12477593>. The dendrogram on the left shows the phylogenetic relationships between the OTUs.

at the figshare URL above). Its relative frequency decreased as the beetles completed their life cycle (showing a peak on day 5) and was highest within the galleries (see Fig. S31 at the figshare URL above). While the synthesis of DSF (*rpfB/rpfF*/DSF system) could be achieved by 35 out of 39 OTUs, only *Stenothrophomonas* may have had the sensing proteins (see Fig. S34 at the figshare URL above). The relative frequency of this OTU increased during the beetles' life cycle, exhibiting a peak in galleries by day 30 (see Fig. S31 at the figshare URL above). The synthesis of GBAP (*fsrD*/GBAP system) could be accomplished by *Enterococcus*, and the sensing proteins might have been present in *Enterococcus* and *Streptococcus* (see Fig. S30 at the figshare URL above), although both were not part of the core bacterial community. The QseC/AI-3 system showed a peak on day 10 in eggs (see Fig. S31 at the figshare URL above)—possibly as a result of the predominant *Enterobacter*. Overall, analyses of the genes involved in biofilm production indicated that their relative frequencies increased toward the end of the beetles' life cycle, while the relative frequencies of the genes related to the planktonic stage decreased (see Fig. S32 at the figshare URL above).

DISCUSSION

We characterized the fungal and bacterial symbionts associated with *X. affinis* during its life cycle using a metabarcoding approach (for an overview, see Fig. 10). Even though bacteria and yeasts are long known to be common in ambrosia beetle galleries (22, 23), the filamentous fungal symbionts, in particular *Raffaelea* and *Ambrosiella* ambrosia fungi, are regarded as the main source of nutrition for both adults and larvae (1, 25). The role of the rest of the microbial community is relatively unclear, even though positive effects of secondary compounds produced by bacteria or yeasts on bark and ambrosia beetles or their fungal mutualists, respectively, have been found (e.g., references 19, 42, 58, and 59). It has never been investigated in ambrosia beetles,



The most abundant and widely distributed bacterial genera were *Enterobacter* and *Stenotrophomonas*. Both genera have been isolated from other bark and ambrosia beetles (4, 27, 46, 66–70). Their relative abundance negatively correlated with the diversity of bacteria, suggesting that they might be able to structure (i.e., dominate) the bacterial communities, possibly by secondary metabolites (see Fig. 33 at <https://doi.org/10.6084/m9.figshare.12477593>).

The fungal community. Forty fungal OTUs composed the fungal community, with Saccharomycetales and Ophiostomatales (both Ascomycota) as the most abundant orders. Among these OTUs, the five most abundant OTUs belonged to the genera *Saccharomycopsis*, *Candida*, and *Raffaelea*. These results correspond with the culturing results from other bark and ambrosia beetles (25, 38, 46, 71). Both our metabarcoding and SEM visualizations showed that the yeasts are dominant in young galleries, after which filamentous *Raffaelea* species follow. This is a surprising finding, because the filamentous ambrosia fungi (in the *Raffaelea* and *Ambrosiella* genus) are usually regarded as the main food fungi of ambrosia beetles (12, 25). Yeasts are common associates of bark and ambrosia beetles, even though their role is poorly understood (18, 58). A recent study found, however, species-specific associations of yeasts with *Raffaelea*-farming scolytine ambrosia beetles (32), which suggests mutualistic (or parasitic) coevolution. Interestingly, this study reported a *Candida berthetii* isolate to be specific to our study species, *X. affinis*, which we also determined as one of the most abundant yeasts in our samples (32). In our study, the relative abundance of *C. berthetii* peaked in the heads of adult female offspring on day 30, when these females are about to leave the nest. This may suggest that this yeast is vertically transmitted to new nests in oral mycetangia of nest foundresses. The presence of *C. berthetii* within the mycetangia of *X. affinis* has also been reported by the culturing study mentioned above (32). All these findings agree with an old hypothesis of yeasts being pioneer colonizers that assist with the preparation of the niche for the growth of the filamentous *Raffaelea* ambrosia fungi (23, 72).

Both our LM and SEM images and the molecular data confirmed that *Raffaelea* fungi appeared within galleries after the hatching of eggs (day 10 versus day 5), which indicates that yeasts are the primary food source at least for the early instars of larvae and possibly also for the egg-laying mother. Furthermore, our molecular data showed that both yeasts were common in the larvae and abdomens of surface-cleaned foundresses, in particular from young nests. This finding is new for scolytine ambrosia beetles, because all previous studies described the filamentous *Raffaelea* or *Ambrosiella* fungi as the principal food source for both larval and adult ambrosia beetles (37, 38, 53, 73). It confirms findings from a culturing study on the platypodine ambrosia beetle, *Platypus cylindrus*, however, in which galleries a yeast, *Endomycopsis platypodis*, established before the primary *Raffaelea* fungus (74). The *Raffaelea* fungi probably serve as a food source after 10 to 15 days. Between days 25 and 30, our SEM pictures showed many cropped conidiospores of *Raffaelea*, which might suggest that the reproduction of conidia declines around that time. This also coincides with the time when the preemerging females load their mycetangia with fungal propagules (likely yeasts and *Raffaelea* conidia) that they transmit to newly founded galleries (24, 43, 44). At that time, yeasts and bacteria were found in layers at the bottom below the *Raffaelea* conidiophores (Fig. 5), possibly suggesting some metabolic division of labor in enzymatic degradation of the wood between the different microbes.

Putative metabolic functions. Ambrosia beetles obviously farm primary ambrosia fungi such as *Raffaelea* and possibly yeasts (see above), which have been thought to degrade the wood surrounding the beetle galleries (e.g., references 39 and 75). Our KEGG analysis allowed us to predict the metabolic functions of about 60% of the bacterial OTUs. Most importantly, this analysis and the fungal genome comparisons included all the core bacterial and fungal OTUs, so it is likely that our analysis covers the most important metabolic functions. Overall, it suggested that the bacterial microbiome may be able to assist in wood and fungal biomass degradation. This is indicated by the four most abundant bacterial OTUs being jointly capable to fully degrade all the fungal and plant polymers except glucan, mannan, and pectin, whereas the five most abundant fungi can fully degrade only glucan and cellulose and partly degrade hemicellulose (Fig. 6 and 7). Whether the degradation of these polymers by bacteria plays an important nutritional role for the ambrosia beetles needs to be determined in future studies.

The bacterial genera *Enterobacter* and *Stenotrophomonas* are particularly abundant during the first days of gallery development, followed by the yeasts and the *Raffaelea* ambrosia fungi. We hypothesize that plant cell wall degradation is carried out initially by the bacterial and yeast microbiome, supplementing carbohydrates for the *Raffaelea* fungi. After day 10, this function is performed jointly by the filamentous fungi, yeasts, and bacteria. The latter are found particularly along the woody surface of the wall, at the bottom of the *Raffaelea* fungus layer that covers the gallery walls (Fig. 5). The breakdown of complex sugars like cellulose, hemicellulose, and pectin first peaked around days 10 to 15, which coincides with a high energy demand of the growing fungi and a strong increase in the number of larvae. A second peak of sugar breakdown was observed around day 30, coinciding with the emergence of the F1 generation. Energy demands around that time are probably very high because preemerging adult female offspring fill their mycetangia (43, 75), build up fat reserves for dispersal (76), and produce juvenile hormone (77). The bacterial genera *Enterobacter* and *Stenotrophomonas* are particularly abundant during the first days of gallery development, followed by the yeasts and *Raffaelea* ambrosia fungi. We hypothesize that plant cell wall degradation is carried out initially by the bacterial and yeast microbiome, supplementing carbohydrates for the *Raffaelea* fungi. After day 10, this function is performed jointly by the fungal and bacterial microbiomes. The highest KO degradation relative frequency picks of the complex sugars (cellulose, hemicellulose, and pectin) took place around day 10 and day 15, when the fungal community and the larval population increased, which would lead to a larger demand of energy. In addition, at day 30, an increase in the abundance of genes involved in wood degradation was observed again; this concurred with the emergence of the F1 generation from the galleries, raising again the energy requirements due to flight and the unknown time in which the F1 females are in starvation mode after leaving the colonies. Li and collaborators (109) established the mycetangia dynamics in *Xylosandrus* species, finding that new females fill their mycetangia with the fungal symbionts right before dispersal (109). Accordingly, the fungal population increases during this period. This feeding behavior results in the increase of the fat content (76) required for the development of the exoskeleton, reproductive organs, and wing muscles (110) and in the stimulation of juvenile hormone production (78) and other pheromones (111, 112), as well as allowing the female to survive during the starvation period. Simple sugars resulting from the degradation of complex sugars on day 30 in preemergence females would be subsequently degraded in the initial stages of the new colony, as observed in day 5 in foundress females.

Wood is a poor source of nitrogen and nitrogenous compounds such as essential amino acids, cofactors, and vitamins. The latter act as cofactors needed for all kind of enzymatic functions (78). Hence, wood-feeding insects generally need to establish a mutualism with microorganisms to supply them with nitrogen, amino acids, and vitamins (79). Currently, it is believed that bark and ambrosia beetles associate with fungi that supply them with all essential compounds (24), for example, by translocation and concentration of nitrogen and other trace elements from within the wood toward the beetle galleries (80). On the basis of our results, it is possible, however, that in addition to the potential translocation of nutrients by the fungi, atmospheric nitrogen fixation may be present within galleries, most likely by a predominant *Enterobacter* OTU and possibly by other less common bacteria. These bacteria might be the ones observed at the bottom of the *Raffaelea* layers, which might ensure anoxic conditions, which are essential for nitrogen fixation to take place. *Enterobacter* dominates galleries, particularly during the establishment of the colony and might boost nitrogen supply for both fungi and beetles in this nitrogen-poor environment. Putative nitrogen-fixing bacteria have been also isolated from other bark beetles (81–83). If this hypothesis can be confirmed in future studies, it would show that all cases of fungal agriculture in nature (humans, ants, and termites) are dependent on nitrogen-fixing bacteria (7, 8).

Given the nitrogen supply, the core bacterial players are possibly able to produce all the amino acids. They may thus provide methionine to fungi and beetles that they are unable to produce it themselves. All the other amino acids could be synthesized by

either the core bacterial or core fungal symbionts. Many of the OTUs that can possibly synthesize essential amino acids increased in abundance during beetle development and were higher within adults and immature offspring than in galleries. This suggests that they are present as gut symbionts and play a nutritional role that increases in importance during development. Furthermore, the core bacteria may supply the beetle diet with several cofactors and vitamins that the core fungi cannot produce (e.g., pantothenate, biotin, and folate).

Quorum sensing is a communication system that enables bacteria to regulate gene expression in response to cell population densities, resulting in phenotypes and physiological responses that allow bacteria to thrive under different conditions. Our analyses suggest that it is possibly present in some of the bacterial symbionts and may induce the yeasts and *Raffaelea* fungi to switch from mycelial to yeast-like growth (Fig. 4). The proximate mechanisms underlying the nutritionally essential induction of yeast-like “ambrosial growth” in ambrosia fungi (40, 41) is one of the major open questions in the ambrosia beetle-fungus mutualism. Other Ophiostomatales fungi are known to switch growth form due to environmental stimuli (84–86), but it is also possible that the OTUs of quorum-sensing bacteria like the *Enterobacter* or the *Stenotrophomonas* may act as triggers (see Fig. S30, S31, and S32 at <https://doi.org/10.6084/m9.figshare.12477593>). It would be worth isolating these bacteria and testing them in interaction assays with the *Raffaelea* ambrosia fungi.

Conclusion. Studies on the ambrosia beetle-fungus symbiosis usually focus on the beetles and their filamentous fungal associates but largely neglect other microbes such as yeasts and bacteria (1, 18, 25). Here we show that yeasts and bacteria are particularly common in young galleries, at the bottom of *Raffaelea* growth, and within the bodies of foundresses and offspring. We also show that these yeasts and bacteria have capabilities in degrading plant polymers, in fixation of atmospheric nitrogen, and in the production of amino acids, cofactors, and vitamins that the filamentous fungi miss. This suggests that yeasts and bacteria have an underappreciated role for ambrosia beetles and their *Raffaelea* fungal mutualists to assist their growth, especially early in gallery development. These findings are corroborated by a recent study that showed species-specific associations between ambrosia fungi and yeasts (including *Candida* and *X. affinis* [32]). Experiments testing the roles of specific yeasts and bacteria can be expected to provide promising results. Overall, it is very likely that the ambrosia beetle-fungus mutualism will soon turn out to be a multipartite symbiosis with additional yeast and bacterial players. This study lists a few candidate microorganisms whose capabilities and interactions with the beetles and the *Raffaelea* ambrosia fungi need to be studied and tested experimentally.

MATERIALS AND METHODS

Study species. *Xyleborus affinis* Eichhoff is native to the tropical and subtropical Americas and widely distributed in the southeastern United States (87, 88). It was introduced into Africa, Asia, Australia, Europe, and the Pacific Islands, including Hawaii (89, 90). *X. affinis* is extremely polyphagous using a wide variety of host plants (248 species), including angiosperms as well as gymnosperms (90). Similar to other ambrosia beetles in the subtribe Xyleborini, *X. affinis* displays sib-mating, haplodiploidy, sexual dimorphism, and strongly female-biased sex ratios (90). Fertilized females disperse from their natal nest and bore a branching tunnel system in the xylem of dead or unhealthy hosts. Tunnel walls they inseminate with symbionts they transmit in oral mycetangia or their guts (91). *X. affinis* may inhabit and expand the same gallery for multiple generations over several years and is regarded among the most social beetles (90). They exhibit a cooperatively breeding social system, defined by some adult daughters staying and engaging as temporal workers in the maternal nest, which may cobreed and overtake the nest (14). Quite uniquely also, larvae engage in social hygienic tasks (39). Adult males are flightless, and their only function is to fertilize their sisters (92).

Medium preparation, beetle rearing, and sample collection. Beetle rearing medium was prepared by the method of Biedermann et al. (53), using *Persea schiedeana* (Chinini) sawdust. Thirty-six adult female foundresses were individually introduced into rearing tubes. Six colonies (tubes) were dissected every 5 days, i.e., at 5, 10, 15, 20, 25, and 30 days after the initiation of the colony. This captures the whole life cycle of *X. affinis* within artificial rearing tubes, from a single mother that needs to feed on the microbial layers covering the gallery walls to her laying eggs (day 5), the development of first larval instars (day 10), second and third larval instars (days 15 and 20), pupae and adult sons (day 25), and adult daughters (day 30) (Fig. 9). Foundresses and offspring of all life stages (larvae, pupae, not fully sclerotized

(= teneral) males and females, adult males) were counted, and if available, six individuals were pooled and used for microbiome sequencing. The heads and abdomens of foundresses were processed separately to consider variation between gut and oral mycetangia contents. We focused the study on females, because females are the ones that found new galleries and transmit starter cultures of microbes in oral mycetangia. Therefore, it is particularly interesting what microbes are found in the heads of foundresses immediately after gallery foundation (i.e., day 5) and right before adult female emergence (i.e., day 30). A section of the gallery tunnels was collected for microbiome sequencing at each sampling time to cover the development of the microbiome throughout gallery development and beetle life stages. For an overview of the whole sampling scheme, see Fig. 1.

DNA extraction library construction and metabarcoding. DNA extraction was performed following the protocol described by Latorre et al. (93). Sequencing was conducted at FISABIO Service of Sequencing and Bioinformatics (Valencia, Spain). Amplicons of the 16S rDNA V3 region and the 18S rDNA region were generated to determine bacterial and fungal diversity. 18S rDNA region primers were SSUfungiF (5'-TGGAGGGCAAGTCTGGT-3') and SSUfungiR (5'-TCGGCATAGTTATGGTTAAG-3'). DNA libraries were constructed using Nextera XT adapters (Illumina Inc.) and Kappa polymerase (Kappa HiFi Hotstart Ready Mix [catalog no. KK2602; Kappa Biosystems]), and purified using Agencourt Ampure XP magnetic beads (catalog no. A63881; Beckman Coulter). Libraries were pooled to an equimolar concentration and sequenced by MiSeq (reagent kit V3, 600 cycles). The raw data were deposited in NCBI's SRA archive under BioProject accession number [PRJNA561207](https://www.ncbi.nlm.nih.gov/bioproject/PRJNA561207).

Sequence assembly and taxonomic annotation. A total of 8,650,891 paired reads were obtained from 28 high-quality sample libraries for the 16S rRNA marker and 2,691,294 paired reads from 27 high-quality libraries for the 18S rRNA marker (see Table S1 at <https://doi.org/10.6084/m9.figshare.12477593>). PRINSEQ-lite 0.20.4 (94) was used to trim the 3' ends of the raw reads and remove positions with a quality score of <20; reads with a mean quality score of ≥ 20 and a length of ≥ 50 nucleotides were kept. Paired reads with overlapping ends were joined using the default parameters of the fastq-join tool of the ea-utils package, release 1.1.2-537 (95). Detection and removal of chimeric sequences were done with mothur v.1.25.0 (96), using the Greengenes database (v13_8_99) as the template for the 16S marker (https://greengenes.secondgenome.com/?prefix=downloads/greengenes_database/gg_13_5/); for the 18S rDNA marker, a self-modified version of the QIIME release of the SILVA database v128 was used (97, 98). The modification consisted of clustering 60 new *Raffaelea* sequences extracted from the SILVA repository (<https://www.arb-silva.de/search/>) together with the 16 *Raffaelea* sequences present in the SILVA database. Clustering was performed using the default parameters of vsearch (v2.3.4) (99, 100) and an identity threshold of 0.99. Consensus sequences obtained from each cluster were added to the SILVA database after removing the original *Raffaelea* sequences.

Operational taxonomic units (OTUs) were picked by open-reference command and defined by clustering at 3% divergence (97% similarity) using the Greengenes database (101) and suppressing the lane mask filter step. The resulting OTU table was converted into a .tsv format with Python's biom-format package (v. 2.1.5) (102) to filter OTUs from chloroplast, archaeal, mitochondrial, and cyanobacterial sequences and remove those with low abundance (five reads or less per sample). To distinguish each OTU in all analyses performed, a unique identifier (ID) was assigned. This unique identifier was defined by an increasing number followed by the OTU ID and the taxonomic annotation (see Table S4 at <https://doi.org/10.6084/m9.figshare.12477593>).

Alpha-diversity analysis and phylogenetic-tree construction. Rarefactions were produced from the filtered OTUs by running the multiple_rarefactions.py script (QIIME v 1.8.0) with the following parameters: $x = 1,500$, $m = 10$, $s = 5$, and $n = 10$. Diversity indexes (observed OTUs, Shannon, Chao1, and Simpson) were calculated, collated, and plotted with scripts of QIIME (v. 1.8.0) (see Fig. S34 and S35 at <https://doi.org/10.6084/m9.figshare.12477593>). The alpha-diversity index and OTU richness were plotted by "vegan" and "stats," and an analysis of variance (ANOVA) and Tukey test were performed to detect significant differences between the diversity indexes across days, body parts, and sample types using R (v.3.3.1).

The visualizations of the bacterial and fungal microbiomes were conducted with the software Graphical Phylogenetic Analysis (GraPhlAn) (103). The relative taxonomic abundances of the samples were displayed with collapsed histograms plotted by "RColorBrewer" and "ggplot2" libraries in R (v.3.3.1). Phylogenetic trees of bacterial and fungal OTUs were constructed using FastTree 2.1.3. (104), by using the script make_phylogeny.py of QIIME 1 (100). The phylogenetic trees were pruned, removing all the OTUs with a relative frequency of <0.1% by the "filter_tree.py" script of Qiime1. The resulting trees were transformed to dendrograms using "ape v5.3" in R (v.3.3.1). To visualize the relative abundances of the most frequent OTUs, we constructed a heatmap for every sample type. We displayed the OTUs using the scripts "ape," "vegan," and "RColorBrewer" in R (v.3.3.1).

Visualization of galleries through microscopy. Samples from the gallery walls were collected for visualization by scanning electron microscopy (SEM) from three galleries, each at days 3, 5, 10, 15, 20, 25, and 30 and for light microscopy (LM) from three galleries, each at days 5, 10, 15, 20, 25, and 30. SEM was done on a FEI Quanta 250 FEG microscope after samples were prepared following the protocol described by Hermida-Montero et al. (105). Light microscopy was done on a DMI 6000B Leica inverted microscope and prepared following the protocol of Guillen et al. (106). Samples from the gallery walls were collected for visualization by scanning electron microscopy (SEM) from 3 galleries each at an age of 3, 5, 10, 15, 20, 25 and 30 days and for light microscopy from 3 galleries each at an age of 5, 10, 15, 20, 25 and 30 days. SEM was done on a FEI Quanta 250 FEG microscope after samples were prepared following the protocol described in Hermida-Montero and collaborators (105). Samples for light microscopy (LM) was

done on DMI 6000B LEICA Inverted Microscope were prepared following the protocol of Guillén and collaborators (106).

Functional metabolic prediction of the bacterial and fungal OTUs. Functional annotations of the bacterial microbiome were conducted with Phylogenetic Investigation of Communities by Reconstruction of Unobserved States (PICRUSt) (version 1.1.3) (107), which allows us to predict bacterial metabolic functions based on 16S rRNA sequences using the Greengenes database of reference genomes. The enrichment analysis of pathways was performed based on the Kyoto Encyclopedia of Genes and Genomes (KEGG) database. We performed the PICRUSt normalization, which is selective for OTUs within the Greengenes database, thus inferring the metabolic profile of 267 bacterial OTUs (with a median of 60,837 reads per sample). This means that a putative metabolic profile could be assigned to about 60% of the bacterial OTUs in our samples.

To illustrate dissimilarities based on KEGG Orthologies (KOs) and L3 KEGG level categories, nonmetric multidimensional scaling (NMDS) across the samples was carried out using the Bray-Curtis distance matrix. The effects of the factors sample type and sampling time on KEGG functional categories were evaluated with a permutational multivariate analysis of variance (PERMANOVA) using a Bray-Curtis dissimilarity matrix that was previously calculated considering the relative abundances of functional categories in all samples. The significance threshold for the PERMANOVA was set at $P < 0.001$. When the PERMANOVA was significant, differences between samples were determined with multiple pairwise comparisons using a Wilcoxon test with Bonferroni correction set at $P < 0.01$. All the analyses were performed using “vegan” and “mass” in R (v.3.3.1). To visualize shared and private KOs between adults, offspring of different life stages, and galleries across development (days 5, 10, 15, 20, 25, and 30), we constructed an UpSet plot using the R package UpsetR (108).

To gain insights into the metabolic potential of the fungi associated with the ambrosia beetles, available genomes of the phylogenetically most closely related fungi ($n = 33$ genomes; see Table S5 at <https://doi.org/10.6084/m9.figshare.12477593>) were selected, and the core genome and their metabolic profile were determined following the methodology reported by Ibarra-Juarez et al. (46). Additionally, the presence of genes and specific metabolic pathways (degradation of plant and fungal cell wall components; biosynthesis of essential amino acids, cofactors and vitamins; nitrogen fixation; quorum sensing and biofilm production) were analyzed and plotted in a heatmap using “ggplot2” and “vegan” for R (v.3.3.1). The main components of the plant cell wall are cellulose, hemicellulose (1,4- β -D-xylan), pectin [poly(1,4- α -D-galacturonide)], lignin (3,4-dihydroxybenzoate), and the simple-sugar components of pectin and hemicellulose, arabinose, and rhamnose. The fungal cell wall consists of chitin (*N*-acetylglucosamine), glucan (1,3- β -glucan), and mannan (1,4- β -mannan). The metabolic pathways for the degradation of these components are given in Fig. S36 at <https://doi.org/10.6084/m9.figshare.12477593>.

To infer the metabolic capability of the bacterial microbiome in specific pathways, the relative frequencies of all genes involved in these pathways were calculated per sample. A boxplot for the sampling times (5, 10, 15, 20, 25, and 30 days) and the type of sample was generated using “ggplot2” and “vegan” in R (v.3.3.1). To analyze the bacterial contribution to the different steps of the selected pathways, we ran the script `metagenome_contributions.py` of PICRUSt (107). This script generates the relative frequency of the KO present in the sample by a specific OTU. We built a stack histogram using the sum of the averages of these relative frequencies of all KOs involved in a metabolic pathway from a specific OTU.

To analyze the capability of the microbiome to produce biofilm, we calculated the relative frequencies per sample of the genes involved in biofilm production and the genes involved in planktonic stage, based on the KOs predicted by PICRUSt. We consider the KOs K00688, K00694, K00703, K00975, K01991, K03087, K03566, K04333, K04334, K04335, K04336, K04761, K06204, K07173, K07638, K07659, K07676, K07677, K07678, K07687, K07689, K07781, K07782, K11531, K11931, K11935, K11936, K11937, and K14051 to be involved in biofilm production and the KOs K02398, K02402, K02403, K02405, K02425, K02777, K03563, K03567, K05851, K07648, K07773, and K10914 to be involved in planktonic stage.

Data availability. The raw data were deposited in NCBI's SRA archive under BioProject accession number [PRJNA561207](https://www.ncbi.nlm.nih.gov/bioproject/PRJNA561207).

SUPPLEMENTAL MATERIAL

Supplemental material is available online only.

FIG S1, TIF file, 0.8 MB.

FIG S2, TIF file, 0.4 MB.

ACKNOWLEDGMENTS

Research reported in this publication was supported by CONACyT-FORDECYT number 292399, Spanish Ministry of Economy and Competitiveness under award numbers SAF2015-65878-R and PGC2018-099344-B-I00, cofinanced by the European Regional Development Fund (ERDF), and from Generalitat Valenciana (project Prometeo/2018/A133). P.H.W.B. was supported by the German Research Foundation (DFG Emmy Noether grant BI 1956/1-1).

Conceptualization, A. Lamelas, L.A.I.-J., G.C., A.M., A. Latorre, and P.H.W.B.; Data curation, A. Lamelas and E.V.; Formal analysis, A. Lamelas, M.A.J.B., D.D., E.I.-L., M.V.-R.-L., G.H.-R., and L.L.; Funding acquisition, A. Lamelas, A.M., P.H.W.B., and A. Latorre; Inves-

tigation, A. Lamelas and L.A.I.-J.; Methodology, A. Lamelas, M.A.J.B., D.D., E.I.-L., M.V.-R.-L., G.H.-R., and L.L.; Project administration, A. Lamelas; Resources, L.A.I.-J.; Software, A. Lamelas, M.A.J.B., D.D., M.V.-R.-L., and E.V.; Supervision, A. Lamelas; Validation, A. Lamelas, M.A.J.B., D.D., E.I.-L., and M.V.-R.-L.; Visualization, A. Lamelas, M.A.J.B., D.D., A.A.-S., and M.V.-R.-L.; Writing – original draft, A. Lamelas, L.C., and P.H.W.B.; Writing – review & editing, A. Lamelas, L.A.I.-J., G.C., E.V., M.A.J.B., D.D., E.I.-L., M.V.-R.-L., G.H.-R., L.L., A.M., A. Latorre, A.A.-S., L.C., P.H.W.B., and D.C.

We declare that no competing interests exist.

REFERENCES

- Biedermann PHW, Vega FE. 2020. Ecology and evolution of insect-fungus mutualisms. *Annu Rev Entomol* 65:431–455. <https://doi.org/10.1146/annurev-ento-011019-024910>.
- Mueller UG, Gerardo NM, Aanen DK, Six DL, Schultz TR. 2005. The evolution of agriculture in insects. *Annu Rev Ecol Evol Syst* 36:563–595. <https://doi.org/10.1146/annurev.ecolsys.36.102003.152626>.
- Biedermann PH, Rohlf M. 2017. Evolutionary feedbacks between insect sociality and microbial management. *Curr Opin Insect Sci* 22:92–100. <https://doi.org/10.1016/j.cois.2017.06.003>.
- Aylward FO, Suen G, Biedermann PHW, Adams AS, Scott JJ, Malfatti SA, Glavina del Rio T, Tringe SG, Poulsen M, Raffa KF, Klepzig KD, Currie CR. 2014. Convergent bacterial microbiotas in the fungal agricultural systems of insects. *mBio* 5:e02077-14. <https://doi.org/10.1128/mBio.02077-14>.
- Currie CR, Scott JA, Summerbell RC, Malloch D. 1999. Fungus-growing ants use antibiotic-producing bacteria to control garden parasites. *Nature* 398:701–704. <https://doi.org/10.1038/19519>.
- Um S, Fraimout A, Sapountzis P, Oh D-C, Poulsen M. 2013. The fungus-growing termite *Macrotermes natalensis* harbors bacillae-producing *Bacillus* sp. that inhibit potentially antagonistic fungi. *Sci Rep* 3:3250–3257. <https://doi.org/10.1038/srep03250>.
- Pinto-Tomás AA, Anderson MA, Suen G, Stevenson DM, Chu FST, Cleland WW, Weimer PJ, Currie CR. 2009. Symbiotic nitrogen fixation in the fungus gardens of leaf-cutter ants. *Science* 326:1120–1123. <https://doi.org/10.1126/science.1173036>.
- Sapountzis P, de Verges J, Rousk K, Cilliers M, Vorster BJ, Poulsen M. 2016. Potential for nitrogen fixation in the fungus-growing termite symbiosis. *Front Microbiol* 7:1993. <https://doi.org/10.3389/fmicb.2016.01993>.
- Aylward FO, Currie CR, Suen G. 2012. The evolutionary innovation of nutritional symbioses in leaf-cutter ants. *Insects* 3:41–61. <https://doi.org/10.3390/insects3010041>.
- Poulsen M, Hu H, Li C, Chen Z, Xu L, Otani S, Nygaard S, Nobre T, Klaubauf S, Schindler PM, Hauser F, Pan H, Yang Z, Sonnenberg ASM, de Beer ZW, Zhang Y, Wingfield MJ, Grimmelikhuijzen CJP, de Vries RP, Korb J, Aanen DK, Wang J, Boomsma JJ, Zhang G. 2014. Complementary symbiont contributions to plant decomposition in a fungus-farming termite. *Proc Natl Acad Sci U S A* 111:14500–14505. <https://doi.org/10.1073/pnas.1319718111>.
- Francoeur CB, Khadempour L, Moreira-Soto RD, Gotting K, Book AJ, Pinto-Tomás AA, Keefover-Ring K, Currie CR. 2019. Bacteria contribute to plant secondary compound degradation in a generalist herbivore system. *bioRxiv* <https://doi.org/10.1101/865212>.
- Hulcr J, Stelinski LL. 2017. The ambrosia symbiosis: from evolutionary ecology to practical management. *Annu Rev Entomol* 62:285–303. <https://doi.org/10.1146/annurev-ento-031616-035105>.
- Biedermann PHW, Taborsky M. 2011. Larval helpers and age polyethism in ambrosia beetles. *Proc Natl Acad Sci U S A* 108:17064–17069. <https://doi.org/10.1073/pnas.1107758108>.
- Biedermann PHW, Klepzig KD, Taborsky M. 2011. Costs of delayed dispersal and alloparental care in the fungus-cultivating ambrosia beetle *Xyleborus affinis* Eichhoff (Scolytinae: Curculionidae). *Behav Ecol Sociobiol* 65:1753–1761. <https://doi.org/10.1007/s00265-011-1183-5>.
- Nuotclà JA, Biedermann PHW, Taborsky M. 2019. Pathogen defence is a potential driver of social evolution in ambrosia beetles. *Proc Biol Sci* 286:20192332. <https://doi.org/10.1098/rspb.2019.2332>.
- Bateman C, Sigut M, Skelton J, Smith KE, Hulcr J. 2016. Fungal associates of the *Xylosandrus compactus* (Coleoptera: Curculionidae, Scolytinae) are spatially segregated on the insect body. *Environ Entomol* 45:883–890. <https://doi.org/10.1093/ee/nvw070>.
- Therrien J, Mason CJ, Cale JA, Adams A, Aukema BH, Currie CR, Raffa KF, Erbilgin N. 2015. Bacteria influence mountain pine beetle brood development through interactions with symbiotic and antagonistic fungi: implications for climate-driven host range expansion. *Oecologia* 179: 467–485. <https://doi.org/10.1007/s00442-015-3356-9>.
- Six DL. 2013. The bark beetle holobiont: why microbes matter. *J Chem Ecol* 39:989–1002. <https://doi.org/10.1007/s10886-013-0318-8>.
- Scott JJ, Oh D-C, Yuceer MC, Klepzig KD, Clardy J, Currie CR. 2008. Bacterial protection of beetle-fungus mutualism. *Science* 322:63. <https://doi.org/10.1126/science.1160423>.
- Cardoza YJ, Klepzig KD, Raffa KF. 2006. Bacteria in oral secretions of an endophytic insect inhibit antagonistic fungi. *Ecol Entomol* 31:636–645. <https://doi.org/10.1111/j.1365-2311.2006.00829.x>.
- García-Fraile P. 2018. Roles of bacteria in the bark beetle holobiont – how do they shape this forest pest? *Ann Appl Biol* 172:111–125. <https://doi.org/10.1111/aab.12406>.
- Haanstad JO, Norris DM. 1985. Microbial symbiotes of the ambrosia beetle *Xyloterinus politus*. *Microb Ecol* 11:267–276. <https://doi.org/10.1007/BF02010605>.
- Francke-Grosman H. 1967. Ectosymbiosis in wood-inhabiting insects, p 141–205. *In* Henry SM (ed), *Symbiosis: associations of invertebrates, birds, ruminants, and other biota*. Academic Press, Cambridge, MA.
- Beaver RA. 1989. Insect-fungus relationships in the bark and ambrosia beetles, abstr 121–143. *In* *Insect-fungus interactions*. 14th Symposium of the Royal Entomological Society of London in collaboration with the British Mycological Society. Academic Press, London, United Kingdom.
- Harrington TC. 2005. Ecology and evolution of mycophagous bark beetles and their fungal partners, p 257–292. *In* Vega FE, Blackwell M (ed), *Insect-fungal associations: ecology and evolution*. Oxford University Press, Oxford, United Kingdom.
- Francke-Grosman H. 1956. Hautdrüsen als Träger der Pilzsymbiose bei Ambrosiakäfern. *Z Morph Okol Tiere* 45:275–308. <https://doi.org/10.1007/BF00430256>.
- Hulcr J, Rountree NR, Diamond SE, Stelinski LL, Fierer N, Dunn RR. 2012. Mycangia of ambrosia beetles host communities of bacteria. *Microb Ecol* 64:784–793. <https://doi.org/10.1007/s00248-012-0055-5>.
- Francke-Grosman H. 1975. Zur epizooischen und endozooischen Übertragung der symbiotischen Pilze des Ambrosiakäfers *Xyleborus saxenisi* (Coleoptera: Scolytidae). *Entomol German* 1:279–292.
- Vanderpool D, Bracewell RR, McCutcheon JP. 2018. Know your farmer: ancient origins and multiple independent domestications of ambrosia beetle fungal cultivars. *Mol Ecol* 27:2077–2094. <https://doi.org/10.1111/mec.14394>.
- Mayers CG, Harrington TC, Masuya H, Jordal BH, McNew D, Shih H-H, Roets F, Kietzka GJ. 2020. Patterns of coevolution between ambrosia beetle mycangia and the Ceratocystidaceae, with five new fungal genera and seven new species. *Persoonia* 44:41–61. <https://doi.org/10.3767/persoonia.2020.44.02>.
- Mayers CG, Bateman CC, Harrington TC. 2018. New *Meredithiella* species from mycangia of *Corthylus* ambrosia beetles suggest genus-level coadaptation but not species-level coevolution. *Mycologia* 110:63–78. <https://doi.org/10.1080/00275514.2017.1400353>.
- Saucedo-Carabez JR, Ploetz RC, Konkol JL, Carrillo D, Gazis R. 2018. Partnerships between ambrosia beetles and fungi: lineage-specific promiscuity among vectors of the laurel wilt pathogen, *Raffaelea lauricola*. *Microb Ecol* 76:925–940. <https://doi.org/10.1007/s00248-018-1188-y>.
- Skelton J, Johnson AJ, Jusino MA, Bateman CC, Li Y, Hulcr J. 2019. A selective fungal transport organ (mycangium) maintains coarse phylogenetic congruence between fungus-farming ambrosia beetles and

- their symbionts. *Proc Biol Sci* 286:20182127. <https://doi.org/10.1098/rspb.2018.2127>.
34. Biedermann PHW, Klepzig KD, Taborsky M, Six DL. 2013. Abundance and dynamics of filamentous fungi in the complex ambrosia gardens of the primitively eusocial beetle *Xyleborinus saxesenii* Ratzeburg (Coleoptera: Curculionidae, Scolytinae). *FEMS Microbiol Ecol* 83: 711–723. <https://doi.org/10.1111/1574-6941.12026>.
 35. Freeman S, Sharon M, Dori-Bachash M, Maymon M, Belausov E, Maoz Y, Margalit O, Protasov A, Mendel Z. 2016. Symbiotic association of three fungal species throughout the life cycle of the ambrosia beetle *Euwallacea nr. fornicatus*. *Symbiosis* 68:115–128. <https://doi.org/10.1007/s13199-015-0356-9>.
 36. Cruz LF, Rocio SA, Duran LG, Menocal O, Garcia-Avila CDJ, Carrillo D. 2018. Developmental biology of *Xyleborus bispinatus* (Coleoptera: Curculionidae) reared on an artificial medium and fungal cultivation of symbiotic fungi in the beetle's galleries. *Fungal Ecol* 35:116–126. <https://doi.org/10.1016/j.funeco.2018.07.007>.
 37. Kajimura H, Hijii N. 1992. Dynamics of the fungal symbionts in the gallery system and the mycangia of the ambrosia beetle, *Xylosandrus mutilatus* (Blandford) (Coleoptera: Scolytidae) in relation to its life history. *Ecol Res* 7:107–117. <https://doi.org/10.1007/BF02348489>.
 38. Cruz LF, Menocal O, Mantilla J, Ibarra-Juarez LA, Carrillo D. 2019. *Xyleborus volvulus* (Coleoptera: Curculionidae): biology and fungal associates. *Appl Environ Microbiol* 85:e01190-19. <https://doi.org/10.1128/AEM.01190-19>.
 39. De Fine Licht HH, Biedermann PHW. 2012. Patterns of functional enzyme activity in fungus farming ambrosia beetles. *Front Zool* 9:13. <https://doi.org/10.1186/1742-9994-9-13>.
 40. Batra LR, Michie MD. 1963. Pleomorphism in some ambrosia and related fungi. *Trans Kans Acad Sci* 66:470–481. <https://doi.org/10.2307/3626545>.
 41. French JRJ, Roeper RA. 1973. Patterns of nitrogen utilization between the ambrosia beetle *Xyleborus dispar* and its symbiotic fungus. *J Insect Physiol* 19:593–605. [https://doi.org/10.1016/0022-1910\(73\)90068-1](https://doi.org/10.1016/0022-1910(73)90068-1).
 42. Grubbs KJ, Surup F, Biedermann PHW, McDonald BR, Klassen J, Carlson CM, Clardy J, Currie CR. 2019. Cycloheximide-producing *Streptomyces* associated with *Xyleborinus saxesenii* and *Xyleborus affinis* fungus-farming ambrosia beetles. *bioRxiv* <https://doi.org/10.1101/511493>.
 43. Schneider I, Rudinsky JA. 1969. Anatomical and histological changes in internal organs of adult *Trypodendron lineatum*, *Gnathotrichus retusus*, and *G. sulcatus* (Coleoptera: Scolytidae). *Ann Entomol Soc Am* 62: 995–1003. <https://doi.org/10.1093/aesa/62.5.995>.
 44. Schneider I. 1976. Untersuchungen über die biologische Bedeutung der Mycetangien bei einigen Ambrosiakäfern. *Material Organismen* 3:489–497.
 45. Carrillo D, Cruz LF, Kendra PE, Narvaez TI, Montgomery WS, Monterroso A, De Grave C, Cooperband MF. 2016. Distribution, pest status and fungal associates of *Euwallacea nr. fornicatus* in Florida avocado groves. *Insects* 7:55. <https://doi.org/10.3390/insects7040055>.
 46. Ibarra-Juarez LA, Desgarennes D, Vázquez-Rosas-Landa M, Villafan E, Alonso-Sánchez A, Ferrera-Rodríguez O, Moya A, Carrillo D, Cruz L, Carrión G, López-Buenfil A, García-Avila C, Ibarra-Laclette E, Lamelas A. 2018. Impact of rearing conditions on the ambrosia beetle's microbiome. *Life (Basel)* 8:63. <https://doi.org/10.3390/life8040063>.
 47. Kostovcik M, Bateman CC, Kolarik M, Stelinski LL, Jordal BH, Hulcr J. 2015. The ambrosia symbiosis is specific in some species and promiscuous in others: evidence from community pyrosequencing. *ISME J* 9:126–138. <https://doi.org/10.1038/ismej.2014.115>.
 48. Kinuura H, Hijii N, Kanamitsu K. 1991. Symbiotic fungi associated with the ambrosia beetle, *Scolytotrupes mikado* Blandford (Coleoptera: Scolytidae)—succession of the flora and fungal phases in the gallery system and the mycangium in relation to the developmental stages of the beetle. *Jpn Forest Soc* 73:197–205.
 49. Kinuura H. 1995. Symbiotic fungi associated with ambrosia beetles. *Jpn Agric Res Q* 29:57–63.
 50. Yang WF, Ye HZ, Zhang M. 2008. Composition and variety of the ambrosia fungi associated with ambrosia beetle, *Xylosandrus germanus* (Blandford) (Coleoptera: Scolytidae). *Acta Entomol Sinica* 51: 595–600.
 51. Rangel R, Pérez M, Sánchez S, Capello S. 2012. Fluctuación poblacional de *Xyleborus ferrugineus* y *X. affinis* (Coleoptera: Curculionidae) en ecosistemas de Tabasco, México. *Rev Biol Trop* 60:1577–1588. <https://doi.org/10.15517/rbt.v60i4.2075>.
 52. Castrejón-Antonio JE, Montesinos-Matías R, Acevedo-Reyes N, Tamez-Guerra P, Ayala-Zermeño MÁ, Berlanga-Padilla AM, Arredondo-Bernal HC, Castrejón-Antonio JE, Montesinos-Matías R, Acevedo-Reyes N, Tamez-Guerra P, Ayala-Zermeño MÁ, Berlanga-Padilla AM, Arredondo-Bernal HC. 2017. Especies de *Xyleborus* (Coleoptera: Curculionidae: Scolytinae) asociados a huertos de aguacate en Colima, México. *Acta Zool Mexicana* 33:146–150.
 53. Biedermann PHW, Klepzig KD, Taborsky M. 2009. Fungus cultivation by ambrosia beetles: behavior and laboratory breeding success in three xyleborine species. *Environ Entomol* 38:1096–1105. <https://doi.org/10.1603/022.038.0417>.
 54. Lofgren LA, Uehling JK, Branco S, Bruns TD, Martin F, Kennedy PG. 2019. Genome-based estimates of fungal rDNA copy number variation across phylogenetic scales and ecological lifestyles. *Mol Ecol* 28:721–730. <https://doi.org/10.1111/mec.14995>.
 55. de Rossi BP, García C, Alcaraz E, Franco M. 2014. *Stenotrophomonas maltophilia* interferes via the DSF-mediated quorum sensing system with *Candida albicans* filamentation and its planktonic and biofilm modes of growth. *Rev Argent Microbiol* 46:288–297. [https://doi.org/10.1016/S0325-7541\(14\)70084-7](https://doi.org/10.1016/S0325-7541(14)70084-7).
 56. Nakayama J, Chen S, Oyama N, Nishiguchi K, Azab EA, Tanaka E, Kariyama R, Sonomoto K. 2006. Revised model for *Enterococcus faecalis* *fsr* quorum-sensing system: the small open reading frame *fsrD* encodes the gelatinase biosynthesis-activating pheromone propeptide corresponding to *staphylococcal* AgrD. *J Bacteriol* 188:8321–8326. <https://doi.org/10.1128/JB.00865-06>.
 57. Weigel WA, Demuth DR. 2016. QseBC, a two-component bacterial adrenergic receptor and global regulator of virulence in *Enterobacteriaceae* and *Pasteurellaceae*. *Mol Oral Microbiol* 31:379–397. <https://doi.org/10.1111/omi.12138>.
 58. Adams AS, Six DL, Adams SM, Holben WE. 2008. In vitro interactions between yeasts and bacteria and the fungal symbionts of the mountain pine beetle (*Dendroctonus ponderosae*). *Microb Ecol* 56:460–466. <https://doi.org/10.1007/s00248-008-9364-0>.
 59. Davis TS, Hofstetter RW, Foster JT, Foote NE, Keim P. 2011. Interactions between the yeast *Ogataea pini* and filamentous fungi associated with the Western pine beetle. *Microb Ecol* 61:626–634. <https://doi.org/10.1007/s00248-010-9773-8>.
 60. Martinson VG, Danforth BN, Minckley RL, Rueppell O, Tingek S, Moran NA. 2011. A simple and distinctive microbiota associated with honey bees and bumble bees. *Mol Ecol* 20:619–628. <https://doi.org/10.1111/j.1365-294X.2010.04959.x>.
 61. Rassati D, Marini L, Malacrinò A. 2019. Acquisition of fungi from the environment modifies ambrosia beetle mycobiome during invasion. *PeerJ* 7:e8103. <https://doi.org/10.7717/peerj.8103>.
 62. Harrington TC, Yun HY, Lu S-S, Goto H, Aghayeva DN, Fraedrich SW. 2011. Isolations from the redbay ambrosia beetle, *Xyleborus glabratus*, confirm that the laurel wilt pathogen, *Raffaelea lauricola*, originated in Asia. *Mycologia* 103:1028–1036. <https://doi.org/10.3852/10-417>.
 63. Dreaden TJ, Davis JM, de Beer ZW, Ploetz RC, Soltis PS, Wingfield MJ, Smith JA. 2014. Phylogeny of ambrosia beetle symbionts in the genus *Raffaelea*. *Fungal Biol* 118:970–978. <https://doi.org/10.1016/j.funbio.2014.09.001>.
 64. Miller KE, Inward DJG, Gomez-Rodriguez C, Baselga A, Vogler AP. 2019. Predicting the unpredictable: how host specific is the mycobiota of bark and ambrosia beetles? *Fungal Ecol* 42:100854. <https://doi.org/10.1016/j.funeco.2019.07.008>.
 65. Malacrinò A, Rassati D, Schena L, Mehzabin R, Battisti A, Palmeri V. 2017. Fungal communities associated with bark and ambrosia beetles trapped at international harbours. *Fungal Ecol* 28:44–52. <https://doi.org/10.1016/j.funeco.2017.04.007>.
 66. Briones-Roblero CI, Hernández-García JA, Gonzalez-Escobedo R, Soto-Robles LV, Rivera-Orduña FN, Zúñiga G. 2017. Structure and dynamics of the gut bacterial microbiota of the bark beetle, *Dendroctonus rhizophagus* (Curculionidae: Scolytinae) across their life stages. *PLoS One* 12:e0175470. <https://doi.org/10.1371/journal.pone.0175470>.
 67. Chung SH, Rosa C, Scully ED, Peiffer M, Tooker JF, Hoover K, Luthe DS, Felton GW. 2013. Herbivore exploits orally secreted bacteria to suppress plant defenses. *Proc Natl Acad Sci U S A* 110:15728–15733. <https://doi.org/10.1073/pnas.1308867110>.
 68. Hernández-García JA, Gonzalez-Escobedo R, Briones-Roblero CI, Cano-Ramírez C, Rivera-Orduña FN, Zúñiga G. 2018. Gut bacterial communities of *Dendroctonus valens* and *D. mexicanus* (Curculionidae: Scolytinae): a metagenomic analysis across different geographical lo-

- cations in Mexico. *Int J Mol Sci* 19:2578. <https://doi.org/10.3390/ijms19092578>.
69. Huang S, Sheng P, Zhang H. 2012. Isolation and identification of cellulolytic bacteria from the gut of *Holotrichia parallela* larvae (Coleoptera: Scarabaeidae). *Int J Mol Sci* 13:2563–2577. <https://doi.org/10.3390/ijms13032563>.
 70. Mason CJ, Hanshaw AS, Raffa KF. 2016. Contributions by host trees and insect activity to bacterial communities in *Dendroctonus valens* (Coleoptera: Curculionidae) galleries, and their high overlap with other microbial assemblages of bark beetles. *Environ Entomol* 45:348–356. <https://doi.org/10.1093/ee/nvv184>.
 71. Dohet L, Grégoire J-C, Berasategui A, Kaltenpoth M, Biedermann PHW. 2016. Bacterial and fungal symbionts of parasitic *Dendroctonus* bark beetles. *FEMS Microbiol Ecol* 92:fiw129. <https://doi.org/10.1093/femsec/fiw129>.
 72. Grossmann H. 1930. Beiträge zur Kenntnis der Lebensgemeinschaft zwischen Borkenkäfern und Pilzen. *Z F Parasitenkunde* 3:56–102. <https://doi.org/10.1007/BF02123692>.
 73. Nakashima T, Goto C, Iizuka T. 1987. The primary and auxiliary ambrosia fungi isolated from the ambrosia beetles, *Scolytus platypus* shogun Blandford (Coleoptera: scolytidae) and *Crossotarsus niponicus* Blandford (Coleoptera: Platypodidae). *J Fac Agric Hokkaido Univ* 63:185–208.
 74. Baker JM, Kreger-van Rij NJW. 1964. *Endomycopsis platypodis* sp.n. (Ascomycetes): an auxiliary ambrosia fungus of *Platypus cylindrus* Fab. (Col. Platypodidae). *Antonie Van Leeuwenhoek* 30:433–441. <https://doi.org/10.1007/BF02046757>.
 75. Lehenberger M, Biedermann PHW, Benz JP. 2019. Molecular identification and enzymatic profiling of *Trypodendron* (Curculionidae: Xyloterini) ambrosia beetle-associated fungi of the genus *Phialophoropsis* (Microascales: Ceratocystidaceae). *Fungal Ecol* 38:89–97. <https://doi.org/10.1016/j.funeco.2018.07.010>.
 76. Atkins M. 1959. A study of the flight of the Douglas-fir beetle, *Dendroctonus pseudotsugae* Hopk. (Coleoptera: Scolytidae). I. Flight preparation and response. *Can Entomol* 91:283–291. <https://doi.org/10.4039/Ent91283-5>.
 77. Tillman JA, Seybold SJ, Jurenka RA, Blomquist GJ. 1999. Insect pheromones—an overview of biosynthesis and endocrine regulation. *Insect Biochem Mol Biol* 29:481–514. [https://doi.org/10.1016/S0965-1748\(99\)00016-8](https://doi.org/10.1016/S0965-1748(99)00016-8).
 78. Hansen AK, Moran NA. 2014. The impact of microbial symbionts on host plant utilization by herbivorous insects. *Mol Ecol* 23:1473–1496. <https://doi.org/10.1111/mec.12421>.
 79. Engel P, Moran NA. 2013. The gut microbiota of insects – diversity in structure and function. *FEMS Microbiol Rev* 37:699–735. <https://doi.org/10.1111/1574-6976.12025>.
 80. Six DL, Elser JJ. 2019. Extreme ecological stoichiometry of a bark beetle–fungus mutualism. *Ecol Entomol* 44:543–551. <https://doi.org/10.1111/een.12731>.
 81. Morales-Jiménez J, Zúñiga G, Villa-Tanaca L, Hernández-Rodríguez C. 2009. Bacterial community and nitrogen fixation in the red turpentine beetle, *Dendroctonus valens* LeConte (Coleoptera: Curculionidae: Scolytinae). *Microb Ecol* 58:879–891. <https://doi.org/10.1007/s00248-009-9548-2>.
 82. Bridges JR. 1981. Nitrogen-fixing bacteria associated with bark beetles. *Microb Ecol* 7:131–137. <https://doi.org/10.1007/BF02032495>.
 83. Peklo J, Satava J. 1949. Fixation of free nitrogen by bark beetles. *Nature* 163:336–337. <https://doi.org/10.1038/163336a0>.
 84. Berrocal A, Oviedo C, Nickerson KW, Navarrete J. 2014. Quorum sensing activity and control of yeast-mycelium dimorphism in *Ophiostoma floccosum*. *Biotechnol Lett* 36:1503–1513. <https://doi.org/10.1007/s10529-014-1514-5>.
 85. Nigg M, Bernier L. 2016. From yeast to hypha: defining transcriptomic signatures of the morphological switch in the dimorphic fungal pathogen *Ophiostoma novo-ulmi*. *BMC Genomics* 17:920. <https://doi.org/10.1186/s12864-016-3251-8>.
 86. Rodríguez-Del Valle N, Rosario M, Torres-Blasini G. 1983. Effects of pH, temperature, aeration and carbon source on the development of the mycelial or yeast forms of *Sporothrix schenckii* from conidia. *Mycopathologia* 82:83–88. <https://doi.org/10.1007/BF00437335>.
 87. Rabaglia RJ, Dole SA, Cognato AI. 2006. Review of American *Xyleborina* (Coleoptera: Curculionidae: Scolytinae) occurring north of Mexico, with an illustrated key. *Ann Entomol Soc Am* 99:1034–1056.2.0.CO;2. [https://doi.org/10.1603/0013-8746\(2006\)99\[1034:ROAXCC\]2.0.CO;2](https://doi.org/10.1603/0013-8746(2006)99[1034:ROAXCC]2.0.CO;2).
 88. Wood SL. 1982. The bark and ambrosia beetles of North and Central America (Coleoptera: Scolytidae), a taxonomic monograph. *Great Basin Naturalist Memoirs* 6:1–1359.
 89. Kirkendall LR. 1983. The evolution of mating systems in bark and ambrosia beetles (Coleoptera: Scolytidae and Platypodidae). *Zoolog J Linnean Soc* 77:293–352. <https://doi.org/10.1111/j.1096-3642.1983.tb00858.x>.
 90. Kirkendall LR, Biedermann PHW, Jordal BH. 2015. Chapter 3. Evolution and diversity of bark and ambrosia beetles, p 85–156. In Vega FE, Hofstetter RW (ed), *Bark beetles*. Academic Press, San Diego, CA.
 91. Schneider I. 1987. Verbreitung, Pilzübertragung und Brutsystem des Ambrosiakäfers *Xyleborus affinis* im Vergleich mit *X. mascarensis* (Coleoptera: Scolytidae). *Entomol General* 12:267–275. <https://doi.org/10.1127/entom.gen/12/1987/267>.
 92. Roeper RA, Treeful LM, O'Brien KM, Foote RA, Bunce MA. 1980. Life history of the ambrosia beetle *Xyleborus affinis* (Coleoptera: Scolytidae) from in vitro culture. *Great Lakes Entomol* 13:141–143.
 93. Latorre A, Moya A, Ayala FJ. 1986. Evolution of mitochondrial DNA in *Drosophila subobscura*. *Proc Natl Acad Sci U S A* 83:8649–8653. <https://doi.org/10.1073/pnas.83.22.8649>.
 94. Schmieder R, Edwards R. 2011. Quality control and preprocessing of metagenomic datasets. *Bioinformatics* 27:863–864. <https://doi.org/10.1093/bioinformatics/btr026>.
 95. Aronesty E. 2011. ExpressionAnalysis ea-utils: command-line tools for processing biological sequencing data. <https://github.com/ExpressionAnalysis/ea-utils>.
 96. Schloss PD, Westcott SL, Ryabin T, Hall JR, Hartmann M, Hollister EB, Lesniewski RA, Oakley BB, Parks DH, Robinson CJ, Sahl JW, Stres B, Thallinger GG, Van Horn DJ, Weber CF. 2009. Introducing mothur: open-source, platform-independent, community-supported software for describing and comparing microbial communities. *Appl Environ Microbiol* 75:7537–7541. <https://doi.org/10.1128/AEM.01541-09>.
 97. Quast C, Priesse E, Yilmaz P, Gerken J, Schweer T, Yarza P, Peplies J, Glöckner FO. 2013. The SILVA ribosomal RNA gene database project: improved data processing and web-based tools. *Nucleic Acids Res* 41:D590–D596. <https://doi.org/10.1093/nar/gks1219>.
 98. Yilmaz P, Parfrey LW, Yarza P, Gerken J, Priesse E, Quast C, Schweer T, Peplies J, Ludwig W, Glöckner FO. 2014. The SILVA and “All-species Living Tree Project (LTP)” taxonomic frameworks. *Nucleic Acids Res* 42:D643–D648. <https://doi.org/10.1093/nar/gkt1209>.
 99. Rognes T, Flouri T, Nichols B, Quince C, Mahé F. 2016. VSEARCH: a versatile open source tool for metagenomics. *PeerJ* 4:e2584. <https://doi.org/10.7717/peerj.2584>.
 100. Caporaso JG, Kuczynski J, Stombaugh J, Bittinger K, Bushman FD, Costello EK, Fierer N, Peña AG, Goodrich JK, Gordon JI, Huttley GA, Kelley ST, Knights D, Koenig JE, Ley RE, Lozupone CA, McDonald D, Muegge BD, Pirrung JR, Reeder J, Sevinsky JR, Turnbaugh PJ, Walters WA, Widmann J, Yatsunenko T, Zaneveld J, Knight R. 2010. QIIME allows analysis of high-throughput community sequencing data. *Nat Methods* 7:335–336. <https://doi.org/10.1038/nmeth.f.303>.
 101. Wang Q, Garrity GM, Tiedje JM, Cole JR. 2007. Naive Bayesian classifier for rapid assignment of rRNA sequences into the new bacterial taxonomy. *Appl Environ Microbiol* 73:5261–5267. <https://doi.org/10.1128/AEM.00062-07>.
 102. McDonald D, Clemente JC, Kuczynski J, Rideout JR, Stombaugh J, Wendel D, Wilke A, Huse S, Hufnagle J, Meyer F, Knight R, Caporaso JG. 2012. The Biological Observation Matrix (BIOM) format or: how I learned to stop worrying and love the ome-ome. *Gigascience* 1:7. <https://doi.org/10.1186/2047-217X-1-7>.
 103. Asnicar F, Weingart G, Tickle TL, Huttenhower C, Segata N. 2015. Compact graphical representation of phylogenetic data and metadata with GraPhlAn. *PeerJ* 3:e1029. <https://doi.org/10.7717/peerj.1029>.
 104. Price MN, Dehal PS, Arkin AP. 2010. FastTree 2 – approximately maximum-likelihood trees for large alignments. *PLoS One* 5:e9490. <https://doi.org/10.1371/journal.pone.0009490>.
 105. Hermida-Montero LA, Pariona N, Mtz-Enriquez AI, Carrión G, Paraguay-Delgado F, Rosas-Saito G. 2019. Aqueous-phase synthesis of nanoparticles of copper/copper oxides and their antifungal effect against *Fusarium oxysporum*. *J Hazard Mater* 380:120850. <https://doi.org/10.1016/j.jhazmat.2019.120850>.
 106. Guillén L, Pascacio-Villafán C, Stoffolano JG, López-Sánchez L, Velázquez O, Rosas-Saito G, Altúzar-Molina A, Ramírez M, Aluja M. 2019. Structural differences in the digestive tract between females and males could modulate regurgitation behavior in *Anastrepha ludens* (Diptera: Tephritidae). *J Insect Sci* 19:7.
 107. Langille MGI, Zaneveld J, Caporaso JG, McDonald D, Knights D, Reyes

- JA, Clemente JC, Burkepille DE, Vega Thurber RL, Knight R, Beiko RG, Huttenhower C. 2013. Predictive functional profiling of microbial communities using 16S rRNA marker gene sequences. *Nat Biotechnol* 31: 814–821. <https://doi.org/10.1038/nbt.2676>.
108. Lex A, Gehlenborg N, Strobel H, Vuilleumot R, Pfister H. 2014. UpSet: visualization of intersecting sets. *IEEE Trans Vis Comput Graph* 20: 1983–1992. <https://doi.org/10.1109/TVCG.2014.2346248>.
109. Li Y, Ruan Y-Y, Stanley EL, Skelton J, Hulcr J. 2019. Plasticity of mycangia in *Xylosandrus ambrosia* beetles. *Insect Sci* 26:732–742. <https://doi.org/10.1111/1744-7917.12590>.
110. McNee WR, Wood DL, Storer AJ. 2000. Pre-emergence feeding in bark beetles (Coleoptera: Scolytidae). *Environ Entomol* 29:495–501. <https://doi.org/10.1603/0046-225X-29.3.495>.
111. Seybold SJ, Quilici DR, Tillman JA, Vanderwel D, Wood DL, Blomquist GJ. 1995. De novo biosynthesis of the aggregation pheromone components ipsenol and ipsdienol by the pine bark beetles *Ips paraconfusus* Lanier and *Ips pini* (Say) (Coleoptera: Scolytidae). *Proc Natl Acad Sci U S A* 92:8393–8397. <https://doi.org/10.1073/pnas.92.18.8393>.
112. Vanderwel D. 1994. Factors affecting pheromone production in beetles. *Arch Insect Biochem Physiol* 25:347–362. <https://doi.org/10.1002/arch.940250409>.